ARTICLE IN PRESS

European Journal of Operational Research xxx (xxxx) xxx

Contents lists available at ScienceDirect

European Journal of Operational Research

journal homepage: www.elsevier.com/locate/ejor

Production, Manufacturing, Transportation and Logistics

# Vehicle routing in precooling logistics with dynamic temperature-dependent product quality decay

Na Lin [a,b], Argyris Kanellopoulos [c], Renzo Akkerman [c,*], Jianghua Zhang [d], Junhu Ruan [a]

[a] School of Economics and Management, Northwest A&F University, Yangling 712100, China
[b] School of Economics and Management, Dalian University of Technology, Dalian 116024, China
[c] Operations Research and Logistics group, Wageningen University, Wageningen 6706 KN, The Netherlands
[d] School of Management, Shandong University, Jinan 250100, China

ARTICLE INFO

*Keywords:*
Logistics
Temperature-dependent quality
Heterogeneous service
Perishable product
Precooling

ABSTRACT

This study focuses on precooling operations for post-harvest fruits and vegetables in smallholder countries, aiming to provide an effective way to reduce product losses in the early stage of food supply chains. In this study, we consider the traditional centralized precooling and emerging mobile precooling to fulfill a series of small-scale and scattered precooling requests, with the goal of minimizing the total operating cost while guaranteeing the product quality of farmers. The resulting problem is a variant of the classic heterogeneous fleet vehicle routing problems with time windows, with the additional consideration of heterogeneous service and temperature-dependent product quality decay. The vehicle routing model is formulated by integrating product quality as a constraint in which a dedicated function is developed to capture the quality dynamics under changing temperatures. We design an improved adaptive large neighborhood search method to solve this problem by identifying a strategy that is able to deal with the interactions among decisions. Experiment results quantify the advantages of managing product quality in the early stage of supply chains for perishable products and provide management insights on conducting quality-based precooling services. Numerical experiments based on small-scale instances of the studied problem as well as large-scale benchmark instances verify the effectiveness and efficiency of the proposed algorithm by comparing it with CPLEX and three state-of-the-art algorithms.

## 1. Introduction

Post-harvest quality loss of fruits and vegetables is a main cause of food waste in many countries (Lejarza & Baldea, 2022). According to Gustavsson et al. (2011), in developing countries, 20-30% of fruits and vegetables are wasted in the food supply chain. The post-harvest first mile (PHFM), i.e., the period after harvesting and before cold storage (or refrigerated transportation), is a key stage that causes food waste (Duan et al., 2020; Gomez-Lagos et al., 2021). Within this stage, the quality of freshly harvested perishable products decays fast over time under the influence of field heat (Blackburn & Scudder, 2009; Chen et al., 2021). For instance, the sugar content of sweet corn declines significantly if it is not cooled within 2 hours after harvest (Vigneault et al., 2004), and a 4-hour delay between harvesting and precooling was shown to result in a 50% increase in water loss (Pelletier et al., 2011). For the example of melons, according to the data collected by Blackburn and Scudder (2009), it can be calculated that the quality (quantified by sugar level) decreases by 3% within one hour after harvest when the field temperature is 30 °C, while after the cold chain is established, the quality decreases only by 2% within one day. This shows the effectiveness of cold chains in reducing the quality losses of fruits and vegetables, and more importantly, it reflects the significance of managing product quality decay for highly perishable products.

One of the ways to get products in the cold chain faster is to use precooling, a rapid cooling process to remove the field heat of products so that respiration can be diminished (Duan et al., 2020). Conducting precooling operations on freshly harvested fruits or vegetables before transporting them to the market or to cold storage has been proven as an important strategy to reduce food losses, help maintain product quality, and extend product shelf life (Lawrence & Melgar, 2018; Baranyai et al., 2020).

For countries with many smallholder farmers, efficient organization

* Corresponding author.
*E-mail addresses:* yana623@mail.dlut.edu.cn (N. Lin), argyris.kanellopoulos@wur.nl (A. Kanellopoulos), renzo.akkerman@wur.nl (R. Akkerman), zhangjianghua@sdu.edu.cn (J. Zhang), rjh@nwsuaf.edu.cn (J. Ruan).

https://doi.org/10.1016/j.ejor.2024.09.041
Received 20 June 2023; Accepted 23 September 2024
Available online 24 September 2024


Please cite this article as: Na Lin et al., *European Journal of Operational Research*, https://doi.org/10.1016/j.ejor.2024.09.041

and management during the PHFM stage can however be challenging. Smallholder farmers often do not have access to expensive equipment used in precooling operations, nor would it be efficient if they would all have this equipment individually (Zhao et al., 2018; Han et al., 2021). In response, precooling service providers (PSPs) emerge to help smallholder farmers conducting precooling operations. As described by Lin et al. (2023), mobile precooling units can be used to supplement centralized precooling stations, to better serve scattered smallholder farmers and reduce quality losses of products by providing timely precooling services. For PSPs, this leads to a challenging optimization problem, i.e., deciding the service sequences for precooling requests considering both mobile precooling and centralized precooling options.

Lin et al. (2023) studied the optimization problem mentioned above, aiming to provide decision support for PSPs. However, their work purely focused on the cost efficiency of the resulting routing problems, and they did not take the detailed dynamics of product quality decay into account. Other literature has studied product quality decay in food supply chains and provided specific formulations to quantify it (e.g., Rong et al., 2011; de Keizer et al., 2017; Stellingwerf et al., 2021). However, most of this literature focuses on the later stages of the supply chain, in which perishable products are mainly stored or transported in cold chains with well-controlled temperatures. In the PHFM stage, however, the temperature is not controlled (yet), and it is often significantly higher and changing over time. This time-varying temperature also leads to dynamic quality decay rates. Quantifying these dynamic product quality changes in the PHFM stage and considering them in the planning and scheduling of PHFM transportation activities is therefore an important problem that has not been addressed before. Integrating dynamic product quality decay into a vehicle routing model that also needs to consider a heterogeneous vehicle fleet and time windows (i.e., a HFVRPTW) generates several challenges: (1) The product quality considerations add additional interactions between decisions in an already complex VRP variant; (2) Dynamic decay rates cause nonlinear quality changes that further complicate the underlying vehicle routing model.

The aim of this paper is to develop a modeling approach to integrate dynamic product quality decay into a typical post-harvest vehicle routing problem, as well as develop a solution approach that considers the product quality dynamics. The contributions of this research mainly focus on the following three aspects: (1) The development of a dedicated function to quantify the quality deterioration of highly perishable products and integrate it into the vehicle routing model, resulting in a new variant of the HFVRPTW considering heterogeneous service and temperature-dependent quality (HFVRPTW-HSTQ); (2) The design of a QTDD-based adaptive large neighborhood search (ALNS) algorithm that leverages the complementary nature of facilities' service capabilities for order fulfillment by identifying the interactions among four attributes of orders (Q: Product Quality; T: Time window; D: Demand; D: Distance), presenting a new tool for solving routing problems of highly perishable products within heterogeneous precooling facilities; (3) The quantification of the advantages of managing product quality in the post-harvest first mile for highly perishable products, providing management insights on conducting quality-based precooling services.

We verify the effectiveness of the proposed ALNS algorithm by comparing our results with the results of CPLEX and three state-of-the-art algorithms. Using the case study of sweet corn, we verify the significance of integrating product quality into the post-harvest logistics. Also, we demonstrate with both qualitative and quantitative evidence that our quality modeling method can bring substantial benefits from an economic and quality point of view when compared to a simplified version that simply uses average temperature data.

The remainder of the paper is organized as follows. Section 2 reviews related work regarding precooling operations and its challenges as well as the integration of product quality in the management of transportation. Section 3 presents the mathematical model of the HFVRPTW-HSTQ (which we will replace with PQ in the following text), in which the quality modeling approach is highlighted. Section 4 describes the designed QTDD-based ALNS algorithm for solving the problem. Section 5 provides numerical experiments, followed by discussion in Section 6. Section 7 summarizes our work and highlights main findings.

## 2. Literature review

### 2.1. Precooling operations and its challenges

Precooling logistics are executed using distinct operation modes in various scenarios. One of the most common precooling operation modes involves utilizing trucks to transport harvested agricultural products from the field to a centralized precooling station (Blackburn & Scudder, 2009; Mercier et al., 2017). While centralized precooling is efficient for handling large-batch precooling demands, it is not suitable for small-batch and scattered demands. In recent years, a more flexible precooling operation mode known as mobile precooling has emerged in developing countries to effectively serve a large number of smallholders (Rodriguez, 2021; MOA, 2023). Mobile precooling vehicles serve several farms within their maximum working hours, requiring well-planned service routes or farm service sequences to reduce travel costs and timely meet growers' precooling needs (Lin et al., 2023).

Comparing the two operation modes, the complexity of the precooling logistics problem primarily stems from the fragmented, diverse, small-scale precooling demands and varied precooling facilities that are often found in developing countries. However, the progress of cold chain development based on precooling in these countries is relatively slow, and has only recently received attention in the literature. Zhu et al. (2023) investigated the network design problem of precooling logistics for fresh agricultural products. Key considerations encompass capacity planning and location selection of cold storage facilities, and optimization of truck routes connecting production areas to cold storage facilities. Li et al. (2022) proposed a location-routing model to optimize the precooling service network for fresh agricultural products, considering centralized facilities and mobile facilities. The primary decision variables encompass the type and capacity of precooling facilities, the locations of centralized facilities, as well as the quantity and routes of vehicles. Lin et al. (2023) tackled a complex precooling logistics optimization problem and developed a customized neighborhood search algorithm to generate service plans for both centralized precooling and mobile precooling simultaneously. Additionally, they offered insights to decision makers on how to reduce operational costs. Wang et al. (2024) introduced the concept of collaborative optimization to the PHFM stage for fruits and vegetables, addressing a synchronized scheduling problem involving mobile grading and precooling vehicles.

The aforementioned studies have started addressing the challenges of precooling station locating and service route planning within precooling logistics. Two studies specifically focused on the integration of centralized precooling and mobile precooling, which is also the primary concern in the current study. However, these studies have not explicitly considered product quality, which is crucial in precooling operations for highly perishable products (Kitinoja & Thompson, 2010; Pelletier et al., 2011). Integrating product quality decay into precooling operations leads to new challenges, including modeling the quality decay process of products under time-varying temperatures and dealing with the implications of quality decay on service plans within heterogeneous precooling facilities. The subsequent section provides a review of research on the integration of product quality within transportation and distribution, aiming to offer insights into addressing the challenges in precooling logistics.

### 2.2. Integrating product quality in transportation and distribution

Existing studies regarding the integration of product quality decay in food distribution and transportation mainly focus on the later stages of supply chains (Akkerman et al., 2010; de Keizer et al., 2015; Albrecht & Steinruecke, 2018; Alvarez et al., 2020; Stellingwerf et al., 2021; Lejarza

& Baldea, 2022). In these studies, product quality decay is typically considered in one of two different approaches.

The first approach of modeling product quality is based on the assumption that shelf life of a product is fixed and the quality of the product decays based on a fixed rate that is determined in advance. For example, Amorim and Almada-Lobo (2014) developed a vehicle routing problem model for prepared meals in which product shelf life was assumed to be fixed. The model was used to maximize the remaining shelf lives of products while minimizing total routing cost. Albrecht and Steinruecke (2018) studied the distribution of fresh products from suppliers via warehouses to markets. Product quality was integrated into a planning and scheduling model by setting thresholds for the latest delivery times for certain quality grades. The latest delivery time of the lowest quality grade was equal to the shelf life of the product and the quality grades of products decreased gradually with the time spent for distribution. Alvarez et al. (2020) studied an inventory-routing problem for perishable goods, where a single supplier was responsible for delivering perishable products to a set of customers during a given finite planning horizon. They also used fixed decay rates to represent usable products and defined the age of products in a discrete set of time. A similar approach of modeling product quality was proposed by Alvarez et al. (2022) who studied the impact of perishability on the production-routing problem by integrating age-dependent pricing, in which the age of products directly influenced the sales price. Chen et al. (2021) quantified the quality changes for perishable fresh products in an urban delivery problem. Also here, a fixed deterioration rate was assumed. All these studies apply fixed decay rates to model product quality in the distribution of perishable products, which however neglects the fact that changing environmental conditions during transportation significantly impacts the decay rate of product quality.

Therefore, the second approach of modeling product quality aims to account for changes of the decay rates during transportation and distribution due to variable environmental conditions (such as changing temperatures). de Keizer et al. (2015) proposed a hybrid optimization and simulation method to design a logistics network for perishable products, where product quality was incorporated by defining a constraint that limits the maximum time-temperature sums of transport links, processes, and hub buffers. In subsequent work, de Keizer et al. (2017) proposed a network design model considering product quality decay and product heterogeneity. Product quality was represented by discrete quality levels which decreased under the influence of time and temperature conditions during transport, storage, or processing. Bogataj et al. (2017) proposed a decision support system for the transportation of perishable products from the field to the final customer. Real-time detection of changes in product perishability dynamics could be achieved based on the temperature, humidity, and gas concentration sensors, and then the information was used for accurate rerouting decisions to guarantee the expected quality conditions of products received by the end consumers. Stellingwerf et al. (2021) studied the delivery problem of fresh products on routes with multiple stops, where product quality was influenced by the door openings and resulting temperature fluctuations. In their studies, the modeling approach proposed by Rong et al. (2011) was used to measure quality deterioration in both arcs and nodes, depending on the relevant temperatures. Lejarza and Baldea (2022) proposed an efficient optimal production and distribution planning framework for perishable products by accurate quantification of multiple physicochemical attributes of product quality influenced by environmental conditions. All these studies do include more detailed methods to quantify product quality changes and take environmental conditions into account, but these methods do not capture the dynamics of product quality decay due to continuously changing temperatures, which may be related to the fact that they mostly consider a temperature-controlled cold chain environment.

However, in the PHFM stage, the temperature is not controlled (yet), and can change substantially with time. A new method for accurate quantification of product quality is therefore required to model the temperature changes. Moreover, integrating time-varying temperatures into modeling product quality deterioration provides an alternative for more precise quality management of perishable products. Previous studies (Lejarza and Baldea, 2020; Lejarza et al., 2021) have developed general product quality modeling methods by integrating time-dependent temperatures, laying a solid foundation for our current investigation. The primary focus of these studies is on optimizing tactical decisions within supply chains, while our study focuses on decision-making at the operational level of precooling logistics (specifically on impacts of temperature fluctuations on vehicle routing decisions).

Integrating quality into the transportation problem directly impacts the decision-making process and exhibits varying performance across different scenarios. From a formulation perspective, product quality can be integrated into the cost objective function through waste disposal costs (Rong et al., 2011) or lost sales (Pasandideh et al., 2023), treated as a new objective (Amorim & Almada-Lobo, 2014; Stellingwerf et al., 2021), or included in constraints to restrict minimum quality levels and latest delivery times (Amorim & Almada-Lobo, 2014; Albrecht & Steinruecke, 2018; Chen et al., 2021). Specifically, in the context of delivery problems, decision-makers should prioritize the delivery of orders with higher quality degradation rates to ensure that customer requirements for product quality are met (Amorim & Almada-Lobo, 2014). In production-routing problems, it is typical for decision-makers to sequence the production of less perishable orders before more perishable ones in order to reduce costs associated with product loss (Chen et al., 2009). For inventory-routing problems, order-picking based on the remaining shelf life of products can effectively reduce suppliers' inventory costs (Fikar, 2018). In the current transportation problem involving multi-type facilities, the influence of product quality on the decision-making process becomes increasingly intricate due to interrelated facility type selection, product quality determinations, and order service sequence decisions. An effective solution method is thus necessary to tackle this challenge.

Inspired by the study of Blackburn and Scudder (2009) where quality differences among different picking batches are accurately modeled, in this research we integrate a precise method to quantify product quality decay when conducting precooling logistics in a VRP model. However, their quality modeling method neglects temperature changes during the PHFM stage, and they do not focus on routing decisions which is an important contribution of this research. In the studied routing problem, quality changes of products vary with the environmental temperature, the service type of precooling, and the time of getting the precooling service. A QTDD-based neighborhood search algorithm is proposed to address the routing problem arising from precooling logistics, which incorporates the influence of product quality on routing decisions within heterogeneous services.

## 3. Problem description and model formulation

In this section, we first describe the basic characteristics of the optimization problem (in Section 3.1), which is followed by the introduction of the proposed quality modeling method in Section 3.2. Finally, we give the mathematical model of the studied routing problem (including the quality modeling) in Section 3.3 and analyze the impacts of product quality considerations on decision-making in Section 3.4. Table A1 in Appendix A illustrates the symbols used in model formulation.

### 3.1. Problem description

The studied problem is derived from the practice of precooling operations occurring at the beginning of the perishable product supply chains. PSPs help farmers to conduct precooling operations after harvesting. There are two types of precooling operations: (1) centralized precooling, and (2) mobile precooling. In both types of precooling operations, after precooling, products are returned to farmers as they sell their products to consumers directly, increasingly by using online platforms, which is a widely used service in China (Lin et al., 2023; Han et al., 2021; Ruan et al., 2020). In the case of centralized precooling, a continuous cold chain is established as collecting trucks transport the products to the central station and refrigerated trucks are then used to return products to the farmers, as presented in Lin et al. (2023). In the case of mobile precooling, the cold chain is established after the on-site precooling. The responsibility for inventory management and the quality of products after precooling lies with the farmers. Farmers have the option of directly selling their products to consumers using third-party logistics services based on cold chain infrastructure or storing them in cold storage facilities until favorable market conditions arise, thereby ensuring the continuity of the cold chain after precooling.

The focus of our study is to optimize the precooling operations conducted by PSPs with the consideration of postharvest losses of products from picking to precooling; we do not explore the subsequent storage and distribution issues. Decisions consist of service type selection (i.e., mobile or centralized precooling) for each request, vehicle routing, vehicle scheduling, and fleet composition. These decisions are made in consideration of product quality and subsequently influence it. The resulting problem is a variant of the classic HFVRPTW problem (Liu & Shen, 1999), with the additional consideration of heterogeneous service and temperature-dependent quality, abbreviated as PQ.

Before conducting precooling operations, PSPs collect farmers' precooling demands in advance. In addition to the number of products, PSPs collect farmers' preferred time windows (including the earliest service time and the latest service time) for obtaining precooling services, typically by offering them several time slot choices. Also, farmers are required to provide the period used for picking so that the quality decay of products can be well considered. Product quality will decay from the start of picking and significantly slows down after precooling. PSPs therefore promise farmers that after the precooling service, a certain level of product quality can be guaranteed. PSPs make plans for conducting precooling services with the goal of minimizing the total operating costs while guaranteeing the quality of farmers' products.

Similar to the setting studied by Lin et al. (2023), two kinds of precooling services are used to fulfill farmers' requests. One is centralized precooling in which products are collected using trucks and transported to centralized stations for precooling. The other one is mobile precooling where vehicles can drive to farms for on-site precooling. Vehicles in these two types of precooling services have heterogenous service processes and service rates when fulfilling the requests, which further cause heterogeneity in product quality decay. If vehicles arrive before the earliest service time of farmers, they need to wait, while they are allowed to arrive at the farmer's field after the latest service time (which we however model with corresponding penalty cost). Each collecting truck has a maximum load capacity. Each precooling vehicle has a maximum working duration, and there is no load capacity constraint on it because it conducts on-site services. The central precooling station has a maximum service capacity and a service time window whose span equals the scheduling period. All vehicles depart from the central precooling station and finally return to it, and they are not allowed to arrive at the station after the latest service time or depart from the station before the earliest service time. The product quality of individual farmers after precooling should meet the minimum quality level promised by PSPs. Farmers are assumed to finish picking produce at the earliest service time they have chosen.

Fig. 1 shows an example of the PQ problem, in which centralized and mobile precooling services are provided for a series of dispersed precooling requests by utilizing collecting trucks and precooling vehicles departing from the central precooling station. Each request has the following information that is known before the service: picking period, the earliest service time, the latest service time, the volume of products, and the location of the farm (as indicated by the numbers in the list beside each request). At each request, decisions include service type, vehicle arrival time, waiting time, delay time, and service duration. Additionally, at the central precooling station, decisions refer to vehicle departure and arrival times.

### 3.2. Quantifying product quality decay

According to Chen et al. (2021), under the influence of field heat, the quality of freshly picked highly perishable products decays fast over time following an exponential function, which becomes much slower when the cold chain is established. In our study, the cold chain is established when precooling starts, and we therefore only focus on the quality decay in the period from the start of picking to the start of precooling. In this period, the decay rate of products is typically higher and more dynamic due to time-varying temperatures. Furthermore, additional variability in the quality of products can result from differences in picking time, which means that even at a single farmer location, product quality can vary across different batches. After the cold chain is established and the product is expected to remain in an environment with a more stable temperature, the remainder of quality decay and shelf life are easier to predict and manage.

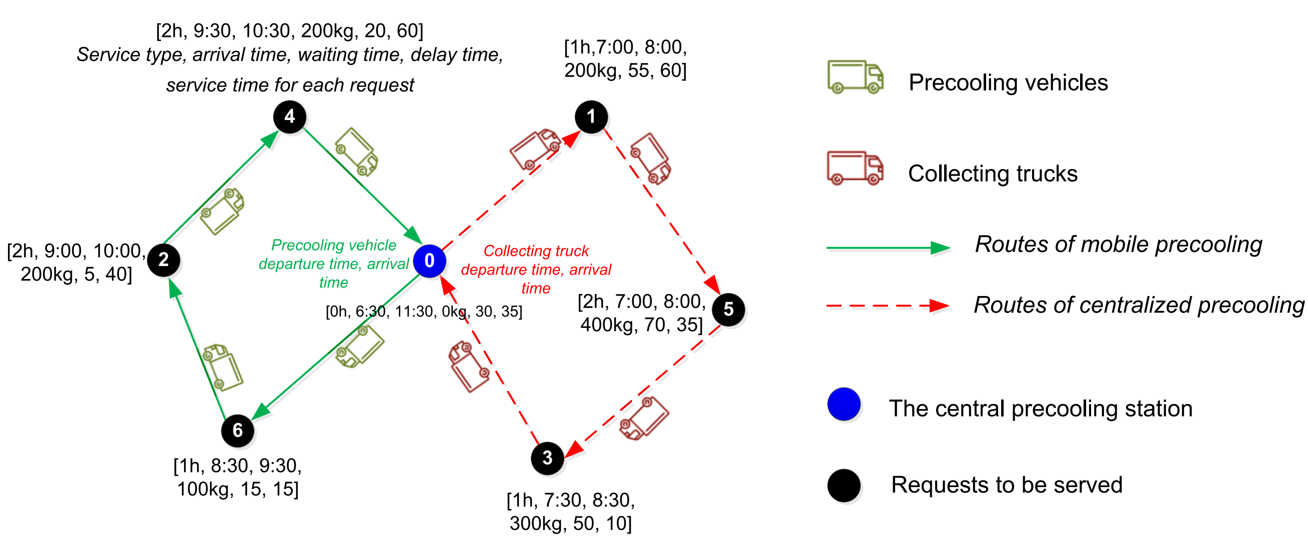


**Fig. 1.** Graphical representation of the PQ problem (the information provided for each request is the picking period, the earliest service time, the latest service time, the volume of products, and the location coordinates).

This study employs the basic exponential function employed by Blackburn and Scudder (2009) for quantifying the quality deterioration of highly perishable products, i.e., $e^{-\alpha\Delta t}$, where $\alpha$ denotes the decay rate of the product and $\Delta t$ denotes the time period. We assume that the quality of all products at the start of picking is 100% and let $\alpha(T(t))$ be the function of the decay rate $\alpha$ of the product with temperature $T$ and time $t$. Then, after a period $\Delta t = [t_1, t_2]$ after picking, the quality of products can be represented by $e^{-\int_{t_1}^{t_2} \alpha(T(t))dt}$.

Let $p_i$ be the picking period of farmer $i$, and then the start time of picking can be represented by $t_i^e - p_i$ since the end time of picking is assumed to equal farmer $i$' earliest service time $t_i^e$. Let $t_i^p$ be the start time of precooling at node $i$. Fig. 2 depicts the quality decay period in both mobile precooling and centralized precooling. As shown in Fig. 2, products decay in the period between the start of picking $t_i^e - p_i$ and the start of precooling $t_i^p$, but the way to calculate $t_i^p$ is different in mobile precooling and centralized precooling. In mobile precooling, $t_i^p$ equals the vehicle $v$'s arrival time at node $i$ plus a possible waiting time and the loading time. In centralized precooling, $t_i^p$ equals the vehicle $v$'s arrival time at the precooling station plus the unloading time of all products serviced by the vehicle.

Similar to Blackburn and Scudder (2009), we also consider the fact that the quality of products that are picked first decays more than those picked later over the picking period. In our method, we use a continual model to capture the quality differences among products that are picked in different times. Product quality $Q_i(t)$ of farmer $i$ at any certain time $t \in [t_i^e, t_i^p]$ declines to $\frac{1}{p_i}\int_{t_i^e-p_i}^{t_i^e}\left(e^{-\int_{t'}^{t} \alpha(T(t''))dt''}\right)dt'$, which sums the quality $e^{-\int_{t'}^{t} \alpha(T(t''))dt''}$ of products that are picked at different times $t' \in [t_i^e - p_i, t_i^e]$. Here normalizing product quality by dividing the picking period $p_i$, $Q_i(t)$ will always be in the interval (0,1) – representing 0 to 100%. When $t$ is equal to $t_i^e$, $Q_i(t)$ represents the initial product quality of famer $i$ before the conduction of precooling operations.

In the following, we verify our modeling approach against one kind of simpler approach to approximate the quality decay: the use of a fixed temperature. We use the data of the sweet corn collected by Blackburn and Scudder (2009) to fit the decay rate function $\alpha(T) = 0.0048e^{0.1036T}$. We also give the temperature function $T(t)$, so that we can illustrate quality changes of the sweet corn with time and temperature, as shown in Fig. 3. In the illustration, hour 8 is the start of precooling.

Fig. 3 depicts product quality changes under changing temperature (as shown by the red curve, $Q(t) = e^{-\int_2^t 0.0048e^{0.1036T(t')}dt'}$) as well as under fixed temperatures $T$ (as shown by blue curves, $Q_T(t) = e^{-(0.0048e^{0.1036T})(t-2)}$). Here it is assumed that products start to decay at time 2. It can be seen that all blue curves based on various levels of the fixed temperatures reflect different quality decay processes from those shown in the curve based on the changing temperatures. Although it is found that in some scenarios the average temperature can be used to approximate the absolute value of quality changes in a period with little deviation from the results of using time-varying temperatures, it is not reliable and may further cause inappropriate decisions. More importantly, the quality change curves under fixed temperatures could not well reflect the real quality decay process with changing temperatures, so it is difficult to provide sufficient product quality information for accurate capture of the variability in quality.

These results show that detailed temperature data play key roles in capturing the variability of product quality, while such data might not always be accessible. In this case, a simplified model considering only average temperatures could be used. However, with the assistance of accurate environmental temperature forecasting and real-time monitoring of product quality, there is promising potential for implementing the proposed quality decay function in practice. These innovative techniques are increasingly being adopted in agricultural production with the rapid development of artificial intelligence and Internet of Things (IoT) technologies (Bogataj et al., 2017; Tsang et al., 2021). In this scenario, detailed temperature information can be forecasted in advance to facilitate initial service planning by decision-makers. For the relatively short-term planning horizon we consider, such temperature forecasts are typically quite accurate. During operations, IoT sensors can be utilized to monitor product quality in real time, allowing for dynamic adjustments to the service plan (Gaukler et al., 2023).

To further explore the effectiveness of the proposed quality modeling approach, we conducted additional theoretical and experimental analyses to compare the performance of the temperature modeling-based method with a simplified version that simply used average temperature data. For more detailed discussions, readers can refer to Appendix C and Section 5.2.

### 3.3. Model formulation

The product quality is integrated into the model developed by Lin et al. (2023) as a constraint that limits the minimum product quality level $Q_{\min}$ of individual requests at the start time of precooling. Since products decay slowly after that point in the chain, $Q_{\min}$ can reflect the quality level of products after the precooling service. Note that one central precooling station and one kind of mobile precooling vehicle are considered in the PQ problem, which is different from the problem studied by Lin et al. (2023) where multi-station and multi-type precooling vehicles are considered.

Eq. (1) guarantees that the product quality $q_i^{\text{start-p}}$ of request $i$ at the start of precooling $t_i^p$ is not less than the minimum level $Q_{\min}$, where $F$ denotes the set of all request nodes. Eq. (2) defines $t_i^p$ in mobile precooling and centralized precooling. In mobile precooling, $t_i^p$ equals the arrival time $a_{iv}^t$ of vehicle $v \in V$ at node $i$ plus a possible waiting time $m_{iv}^t$ and the loading time $bd_i$. In centralized precooling, $t_i^p$ equals the vehicle

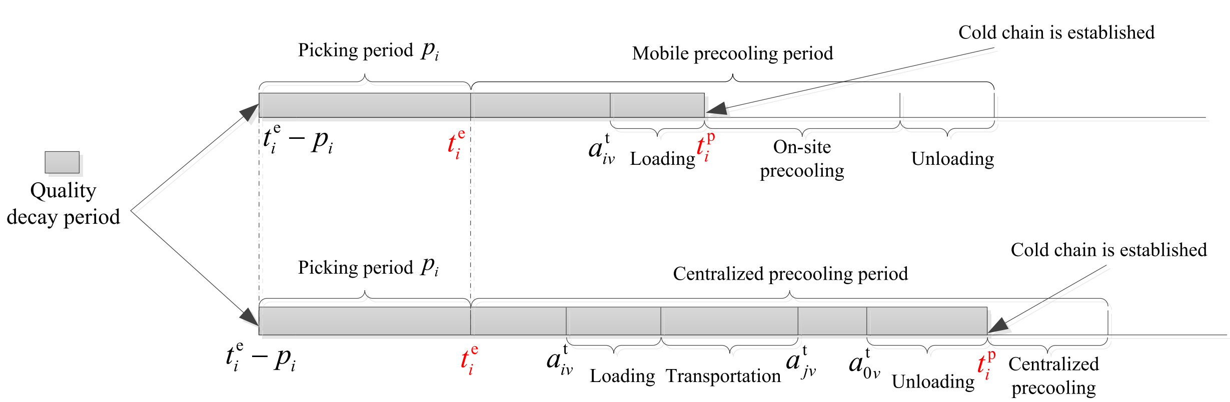


**Fig. 2.** Quality decay period in mobile precooling and centralized precooling.

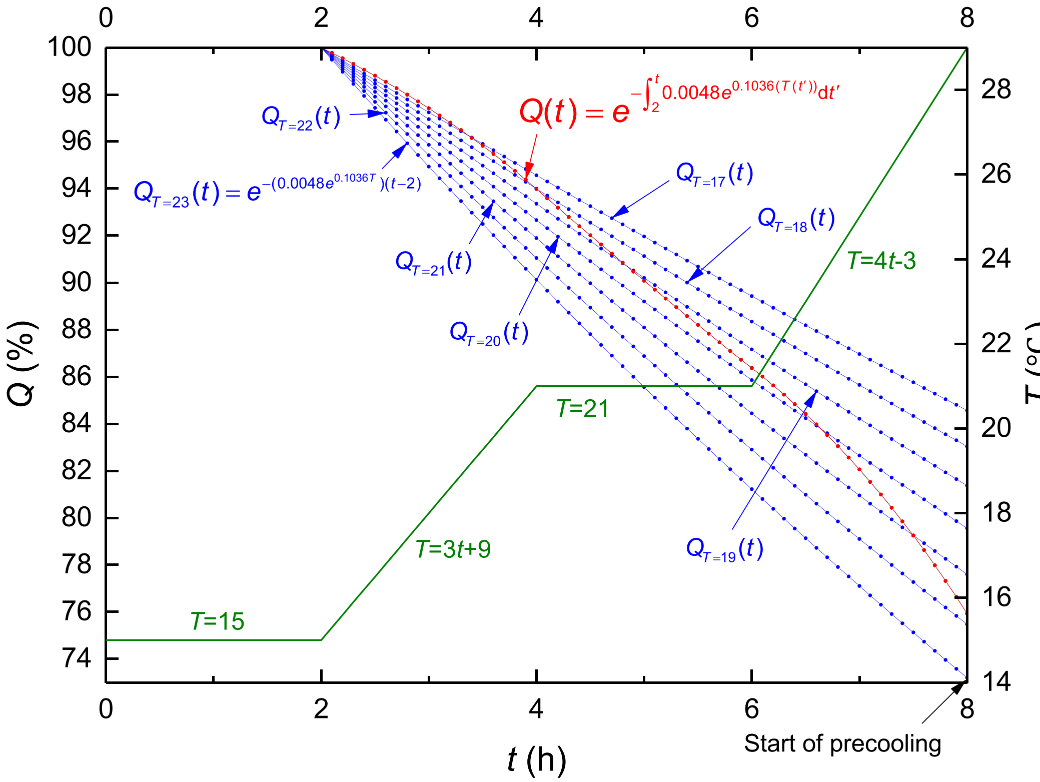


**Fig. 3.** Comparison between quality decay with and without the consideration of changing temperatures.

$v$'s arrival time at the precooling station $a_{0v}^{t}$ plus the unloading time of all products serviced by the vehicle. Here $b$ represents the loading or unloading rate, and $d_i$ shows the product volume of request $i$. $F^0$ denotes the set of all request nodes plus the central precooling station node 0, and $N_v$ denotes the set of request nodes served by vehicle $v$.

$$q_i^{\text{start-p}} = \frac{1}{p_i}\int_{t_i^e - p_i}^{t_i^e}\left(e^{-\int_{t'}^{t_i^p}\alpha(T(t''))\mathrm{d}t''}\right)\mathrm{d}t' \geq Q_{\min} \qquad \forall i \in F \tag{1}$$

$$t_i^{\text{p}} = \begin{cases} a_{iv}^{t} + m_{iv}^{t} + bd_i & \text{if } \sum_{j\in F^0}\sum_{o=2} x_{ijv}^{o} = 1 \\ a_{0v}^{t} + \sum_{j\in N_v} bd_j & \text{otherwise} \end{cases} \qquad \forall i \in F, v \in V \tag{2}$$

Based on the above description, we can formulate PQ as a mixed-integer nonlinear programming model by adding Eqs. (1) and (2) to the model presented in Lin et al. (2023). Due to space limitations, the mathematical formulation of the model is included in Appendix A.

The objective is to minimize the total operating cost, consisting of the total fixed depreciation cost of vehicles, the variable costs based on the travel distance of all vehicles, the total precooling service costs, and the total costs for early or late service at request nodes. The decision variables include binary variables $x_{ijv}^{o}$ indicating whether vehicle $v$ belonging to service type $o$ visits from node $i$ to node $j$, and continuous variables such as the vehicle's arrival time $a_{iv}^{t}$, wait time $m_{iv}^{t}$, delay time $n_{iv}^{t}$, service time $q_{iv}^{t}$ at node $i$, departure time $l_{0v}^{t}$ from the central station, time $t_i^{\text{p}}$ when order $i$ receives precooling service time, and product quality $q_i^{\text{start-p}}$ in order $i$ at time $t_i^{\text{p}}$. Main constraints include the minimum quality level $Q_{\min}$ (Eq. (1)), the definition of the start time of precooling $t_i^{\text{p}}$ (Eq. (2)), basic VRP (vehicle routing problem) constraints, the maximum load capacity of trucks $C_{\text{k}}$, the maximum service capacity of the precooling station $C_{\text{s}}$, the maximum working time of precooling vehicles $T_{\max}$, the latest return time of vehicles to the precooling station $t_0^{\text{l}}$, and domain of decision variables.

### 3.4. Impacts of product quality considerations on decision-making

This section aims to analyze the influence of product quality degradation on the transportation planning procedure of precooling operations, thereby providing insights for algorithm design. The consideration of product quality in precooling logistics causes complex interactions among decision variables. Here, we analyze this complexity in detail from two aspects of order allocation and routing decisions.

The consideration of product quality introduces two additional factors that influence the order allocation decision: the initial quality and service time windows of orders. Specifically, orders with lower initial quality are more likely to be served by mobile precooling, and centralized precooling is more likely to serve orders with higher initial quality. This allocation strategy can fully leverage the timeliness of mobile precooling services and compensate for any delays in centralized precooling operations. Furthermore, according to equation (1), high temperatures can accelerate product quality degradation. If there is an upward trend in temperature during the scheduling period, it can be known that orders with later service start times are more likely to be served by mobile precooling, and centralized precooling is more likely to serve orders with earlier service start times.

In addition to influencing order allocation decisions, product quality considerations have a direct impact on vehicle routing decisions, particularly in centralized precooling. Fig. 4 depicts the truck's routing decisions with the considerations of product quality, where $T_i^{\text{latest}}$

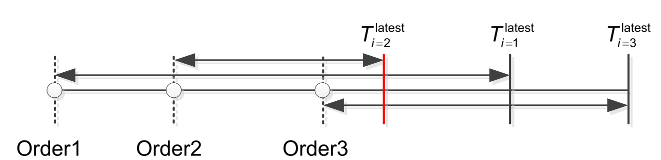


**Fig. 4.** An illustration of the truck's routing decisions with the considerations of product quality.

represents the latest time for order $i$ to receive precooling service to ensure that the quality constraint is met. Since orders can only be precooled after the truck returns to the central station and completes unloading operations, $T_i^{\text{latest}}$ can restrict the return time of the truck and directly affect the its service capacity. As illustrated in Fig. 4, $T_{i=2}^{\text{latest}}$ is earlier than $T_{i=2}^{\text{latest}}$ and $T_{i=2}^{\text{latest}}$, indicating that the truck should return to the station before $T_{i=2}^{\text{latest}}$ to guarantee the quality level of all orders.

Based on the aforementioned analysis, certain insights can be derived for the design of the solution approach. Primarily, it is important to consider the quality attributes of orders in allocation decision-making and ensure that orders are assigned to services aligning with their capabilities. Additionally, accounting for the impact of inserting orders into current routes on vehicles' service capacities has the potential to optimize vehicle routing decisions.

## 4. A QTDD-based ALNS algorithm for the PQ problem

To find effective solutions to the studied problem, a solution approach also needs to explicitly consider heterogeneous services and product quality. Lin et al. (2023) developed a multi-level struct-based solution representation to represent the individual solutions, based on which they also developed customized solution evaluations, feasibility checks as well as neighborhood search heuristics. In this context, the term "struct-based" denotes that the solution is represented by a structure containing a series of data of various types. Their approach considered heterogeneous services but not product quality. In this study, we also use similar solution representations, solution evaluations, and feasibility checks to solve the current problem PQ. However, in PQ, the additional consideration of product quality causes more complex interactions among decision variables (as presented in Section 3.4), requiring a novel customized solution approach for effective resolution.

To solve the PQ problem, we extended the ALNS algorithm by integrating a QTDD (Q: Product Quality; T: Time window; D: Demand; D: Distance) strategy. In QTDD, time windows, demands, and distances are common elements of VRPTW-related problems, but the inclusion of quality considerations leads to a different view on them, as for instance higher demands or far-away customers have to be dealt with in a certain way to ensure quality requirements. These classic routing aspects are therefore also used in specific ways in our solution method. The decision to use all four aspects in the acronym is thus based on the fact that the quality aspect significantly impacts how the other three are considered, and it is important to take an integrated view on these four aspects.

The main point of the QTDD strategy is to exploit the complementary nature of facilities for order fulfillment within heterogeneous services. It can therefore be utilized to make decisions of allocating orders to different services, particularly during the initial stage of the solution generation procedure and in destroy heuristics, as introduced in Sections 4.3 and 4.4.1, respectively, ensuring that facilities are handling orders aligned with their capabilities. Specifically, mobile precooling is effective for serving orders that are farther from the central station with smaller demands, lower initial quality, or later earliest service times (where higher temperatures and faster quality decay occur); whereas centralized precooling applies to the opposite case. The QTDD strategy can also be applied to make routing decisions, particularly in formulating the evaluation function for determining the service sequence of orders. This allows orders with lower insertion cost (including distance-based vehicle variable costs and time-related penalty costs) and smaller impacts on the vehicle's service capacity to be prioritized for insertion (details in Section 4.4.2). We identified that in centralized precooling for trucks, orders' quality dominates the vehicles' service capacity, while for mobile precooling, vehicles' service capacity is mainly influenced by orders' demands. Additionally, the QTDD strategy is integrated into designing a customized improvement procedure to further optimize the routing plan based on local adjustments, as presented in Section 4.5.

In conclusion, compared to the previous literature (Lin et al., 2023), the algorithm presented here contributes the following three novel elements: (1) Proposing a QTDD-based initial solution generation method to obtain high-quality feasible solutions, including customized insertion strategies for both mobile precooling (MP) routes and centralized precooling (CP) routes; (2) Developing destroy heuristics considering the QTDD attributes of orders served by MP and CP, and developed the QTDD-based evaluation functions for repair heuristics; (3) Proposing a two-stage improvement procedure to improve the solution quality based on the QTDD strategy.

In the remainder of this section, we focus on these new QTDD elements, and emphasize the novelty compared to the work by Lin et al. (2023). We first briefly introduce the solution representation and feasibility check. We then introduce the proposed QTDD-based initial solution generation, neighborhood search heuristics, and improvement procedures. Furthermore, we provide two implementing techniques to reduce the time consumed in calculating product quality.

### 4.1. Solution representation

As shown in Fig. 5, a solution is represented by a struct consisting of three parts, including vehicle routing, the arrival time at nodes, and route costs. For the vehicle routing part, a three-level structure is used to represent the solution, including the grand route level, the precooling service level, and the vehicle route level, where MP routes ([1, 4, 7, 3,1], [1, 8, 5, 1]) and CP routes ([1, 6, 2, 1], [1, 9, 1]) are stored separately. The number "1" denotes the precooling station node while numbers "2" to "9" represent the request nodes. Arrival times for two mobile precooling vehicles at nodes are stored in lists [4, 12, 20, 43, 56] and [0, 14, 36, 47], whereas arrival times for two trucks at nodes are stored in lists [5, 18, 35, 50] and [16, 22, 34]. Additionally, the route cost part employs a two-level structure to store costs of routes served by MP and CP.

The current solution representation does not include a list of service types as illustrated in Lin et al. (2023), as this information is already included in the vehicle routing list by storing routes fulfilled by different services separately. Also, in this study, the lists of waiting and delaying time at nodes are removed from the solution representation for further simplification, considering the fact that they do not contribute much to solution evaluations.

### 4.2. Feasibility check

As the feasibility check uses the solution representation, the feasibility check developed by Lin et al. (2023) is also adjusted. If nodes are inserted into MP routes, the feasibility of constraints related to vehicles' return times to the precooling station as well as vehicles' working times are first checked. Then the feasibility of constraints related to the orders' quality levels at the start time of precooling are checked.

If nodes are inserted into CP routes, the feasibility of the service capacity of the precooling station constraint is checked first, followed by the check of trucks' loading capacity. Vehicles' return times to the precooling station as well as orders' quality levels at the start time of precooling are checked in the last step.

### 4.3. QTDD-based initial solution generation

We identify the characteristics of heterogeneous service in fulfilling orders with different attributes and design a QTDD-based initial solution generation. More specifically, we expect that MP will be used to serve those requests that are far away from the central precooling station with low initial quality, later earliest service time, and small-volume products. And that the opposite is the case for CP. This is later also verified in our experiments (see Section 5.1.1). This logic is used in the QTDD-based initial solution generation, illustrated schematically in Fig. 6.

As shown in Fig. 6, two steps are included: order allocation and order insertion. For order allocation, $QTDD_i^{\text{value}}$ is used for preliminary

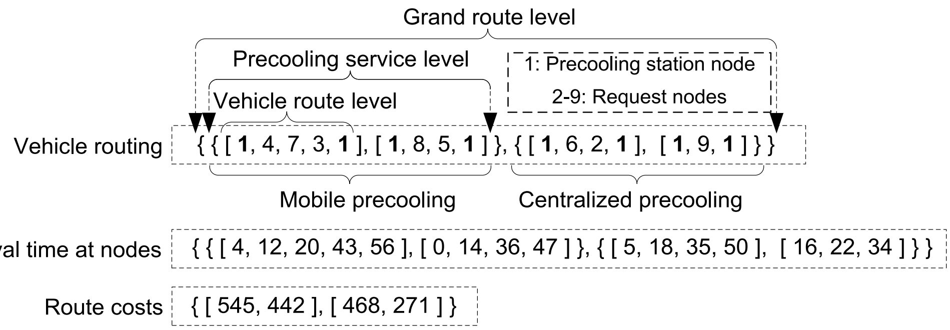


**Fig. 5.** An example of the solution representation.

allocation, as defined by Eq. (3). Here orders with $QTDD_i^{\text{value}}$ values larger than the average value of all orders are primarily allocated to CP, and the remaining orders are allocated to MP. Thus, large-volume orders close to the precooling station with earlier earliest service times and high initial quality are more likely to be served by CP, while MP is the opposite, which is compatible with the service capabilities of MP and CP services.

$$QTDD_i^{\text{value}} = \frac{q_i^{\text{ini}}}{\max_{i \in F} q_i^{\text{ini}}} \bigg/ \frac{t_i^{\text{e}}}{\max_{i \in F} t_i^{\text{e}}} + \frac{d_i}{\max_{i \in F} d_i} \bigg/ \frac{d_{i0}}{\max_{i \in F} d_{i0}} \tag{3}$$

After the preliminary allocation, further adjustments are applied to the allocation result considering related constraints, including: (1) For an order $i$ allocated to MP, if the return time of the vehicle to the precooling station violates the latest time in the case where one MP route only serves one order, remove order $i$ to the set of CP; (2) For an order $i$ allocated to CP, if the product quality at the start time of precooling could not reach the minimum level in the case where one CP route only serves one order, remove order $i$ to the set of MP; and (3) If the service capacity of the precooling station is violated, remove the first $n$ orders with the smallest demand from the set of CP. Assume that $C_{\text{n}}$ represents the total demand of the $n$ orders, $C_{\text{tot}}$ denotes the total demand transported to the precooling station, and $C_{\text{s}}$ denotes its maximum service capacity. Therefore, $n$ is determined as the smallest value such that $C_{\text{n}}$ is greater than or equal to $C_{\text{tot}} - C_{\text{s}}$ .

Order insertion procedure for the MP and CP route is different. For orders $i \in O_{\text{M}}$ from the set of MP, because of long service times, the first order in route $R_{\text{c}}$ served by vehicle $v$ is selected as the order with the earliest $t_i^{\text{e}}$ so that more orders can be served in one route. After that, calculate the insertion cost $I_{jv}^{\text{M}}$ of individual orders from $O_{\text{M}}$ when inserting them to route $R_{\text{c}}$ and choose the order $j$ with the lowest $I_{jv}^{\text{M}}$ as the successor. Here $I_{jv}^{\text{M}}$ is the sum of the waiting cost, delay cost, and travel cost when inserting node $j$ as the successor of node $i$, which reflects the time interval and distance between nodes $i$ and $j$. Then insert order $j$ into route $R_{\text{c}}$ if constraints $T_{\max}$, $a_{0v}^{\text{t}}$, $Q_{\min}$ are respected; Otherwise, generate a new route and repeat the above steps until $O_{\text{M}}$ is empty. For orders $i \in O_{\text{C}}$ from the set of CP, considering the fact that the earlier the order is accessed, the greater the quality losses, the first order in route $R_{\text{c}}$ is selected as the order with the highest initial quality $q_i^{\text{ini}}$ that is equal to the product quality at the end time of picking $Q_i\left(t_i^{\text{e}}\right)$. After that, calculate the inseretion cost $I_{jv}^{\text{C}}$ of all orders from $O_{\text{C}}$. The order $j$ with the minimum $I_{jv}^{\text{C}}/q_i^{\text{ini}}$ is chosen as the successor, meaning that orders with higher initial quality and lower insertion costs are inserted earlier. In this way, more orders can be served in one CP route under the constraint of the minimum quality level, and orders are inserted at good positions with low costs. Then insert order $j$ into route $R_{\text{c}}$ if constraints $C_{\text{k}}$, $a_{0v}^{\text{t}}$, $Q_{\min}$ are respected; Otherwise, generate a new route and repeat the above steps until $O_{\text{C}}$ is empty. Using the QTDD-based initial solution generation, feasible initial routes are generated for MP and CP with low costs.

We have conducted preliminary experiments to test the performance of the QTDD-based initial solution generation approach by comparing it with the sequence-based insertion approach proposed by Lin et al. (2023). Results verified that using the current approach can improve the initial solution by 20% to 30%, and finally contribute to improving the best solution by 5% on average.

### 4.4. Destroy and repair heuristics

#### 4.4.1. Destroy heuristics

The QTDD strategy is integrated into the design of destroy heuristics with four novel destroy heuristics, reflecting the four QTDD attributes. In addition, we also use the efficient worst removal heuristic proposed by Lin et al. (2023), leading to a total of 5 destroy heuristics. Let $n'$ be the number of removed nodes, $L_{\text{r}}$ be the set of removed nodes.

(1) *Initial-quality-related removal* (IQR). Timely services of MP contribute to less product quality losses, so MP is useful to serve those requests with low initial quality levels, and CP is on the opposite case. IQR aims to remove requests with low initial quality levels fulfilled by CP and requests with high initial quality levels fulfilled by MP. The SDR heuristic iteratively removes $|O_{\text{C}}|/|F|n'$nodes $i^*$ from $O_{\text{C}}$ where $i^* = \text{argmin}_{i \in O_{\text{M}} \setminus L_r} q_i^{\text{ini}}$, and $|O_{\text{M}}|/|F|n'$nodes $i^*$ from $O_{\text{M}}$ where $i^* = \text{argmax}_{i \in O_{\text{C}} \setminus L_r} q_i^{\text{ini}}$.

(2) *Earliest-service-time-related removal* (ESTR). Analyzing the results of the experiments, it is found that CP tends to serve orders with earlier $t_i^{\text{e}}$, and MP is on the opposite case. This is because in the tested scenarios, environemnt temperature increases with time during the scheduling. In this case, services happening earlier can cause less quality losses than services happening later. ESTR can be customized considering the environemnt temperature during the scheduling. Taking the increasing temperature as an example, ESTR aims to remove requests with later $t_i^{\text{e}}$ fulfilled by CP and requests with earlier $t_i^{\text{e}}$ fulfilled by MP. The ESTR heuristic iteratively removes $|O_{\text{C}}|/|F|n'$nodes $i^*$ from $O_{\text{C}}$ where $i^* = \text{argmax}_{i \in O_{\text{C}} \setminus L_r} t_i^{\text{e}}$, and $|O_{\text{M}}|/|F|n'$nodes $i^*$ from $O_{\text{M}}$ where $i^* = \text{argmin}_{i \in O_{\text{M}} \setminus L_r} t_i^{\text{e}}$.

(3) *Order-demand-related removal* (ODR). This heuristic considers the demand attribute of orders, aiming to remove large-volume orders from MP routes and small-volume orders from CP routes. The ODR heuristic iteratively removes $|O_{\text{M}}|/|F|n'$nodes $i^*$ from $O_{\text{M}}$ where $i^* = \text{argmax}_{i \in O_{\text{M}} \setminus L_r} d_i$, and $|O_{\text{C}}|/|F|n'$nodes $i^*$ from $O_{\text{C}}$ where $i^* = \text{argmin}_{i \in O_{\text{C}} \setminus L_r} d_i$.

(4) *Station-distance-related removal* (SDR). This heuristic considers the distance attribute of orders, aiming to remove those requests close to the station fulfilled by MP and requests far away from the station fulfilled by CP. The SDR heuristic iteratively removes $|O_{\text{M}}|/|F|n'$nodes $i^*$ from $O_{\text{M}}$ where $i^* = \text{argmin}_{i \in O_{\text{M}} \setminus L_r} d_{0i}$, and $|O_{\text{C}}|/|F|n'$nodes $i^*$ from $O_{\text{C}}$ where $i^* = \text{argmax}_{i \in O_{\text{C}} \setminus L_r} d_{i0}$.

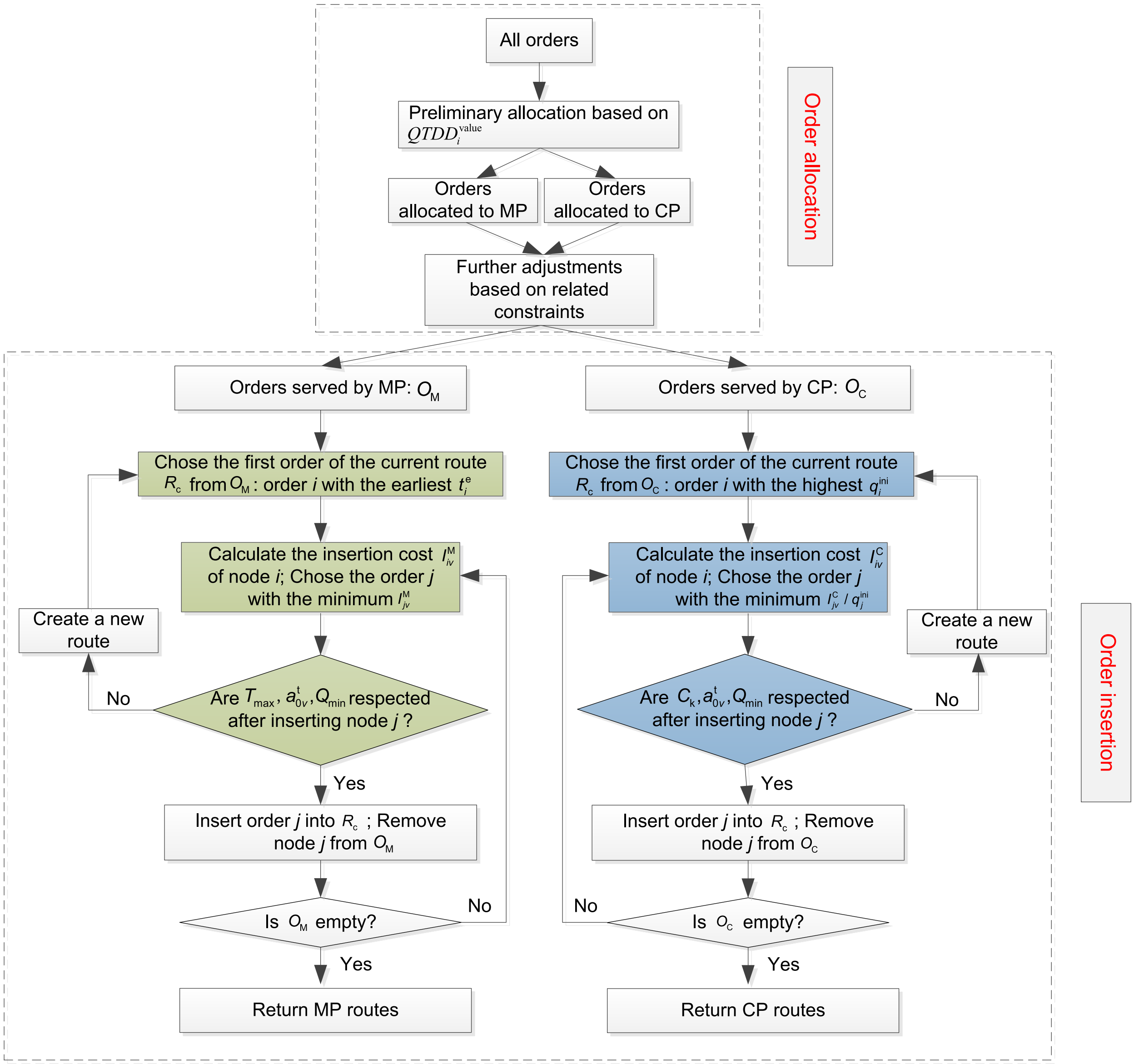


**Fig. 6.** Schematic representation of the QTDD-based initial solution generation approach.

### 4.4.2. Repair heuristics

Two repair heuristics including basic greedy insertion and regret insertion are employed in this study. During each insertion, two steps are included: (1) calculate the insertion costs or regret costs of all removed nodes and (2) choose one node and insert it into the current solution. Feasibility checks and solution evaluations are involved in each calculation of the node's insertion cost. The former is based on the procedure introduced in Section 4.2, while the latter is based on Eq. (4). This evaluation function is developed by integrating the QTDD strategy to calculate the cost of inserting order $i$ into route $R_c$, including the increased travel cost $d_i^{in}$, precooling cost $p_i^{in}$, vehicle's waiting and delay cost $C_{wd\_in}(i, R_c)$, and vehicle's service capacity loss cost $C_v^{cap}$. The calculations for the first three terms are consistent with those in Lin et al. (2023), and the last term is calculated according to Eq. (5). As presented in Eq. (5), $C_v^{cap}$ is represented by the product of vehicle's fixed cost $h_v$ and the loss ratio of its service capacity, where $S_b(i, R_c)$ and $S_a(i, R_c)$ denote the service capacity of route $R_c$ before and after order $i$ is inserted into vehicle $v$. The service capacity of vehicles in the studied problem is defined by Eq. (6) as the duration between their return to and departure from the central station. For trucks in centralized precooling, vehicle $v$'s return time to the central station can be represented as $\min\left(t_0^e, min_{j\in N_v}\left(T_j^{latest}\right) - \sum_{j\in N_v} bd_j\right)$, where $min_{j\in N_v}\left(T_j^{latest}\right) - \sum_{j\in N_v} bd_j$ denotes the latest return time constrained by the minimum quality level. Eq. (6) can also be utilized to represent $S_a(i, R_c)$, with the distinction that the set $N_v$ of order served by vehicle $v$ does not include order $i$.

$$C_{in}(i, R_c) = d_i^{in} + p_i^{in} + C_{wd\_in}(i, R_c) + C_v^{cap} \tag{4}$$

$$C_v^{cap} = h_v * (S_b(i, R_c) - S_a(i, R_c))/S_b(i, R_c) \tag{5}$$

$$S_b(i, R_c) = \min\left(t_0^e, \underset{j\in N_v}{min}\left(T_j^{latest}\right) - \sum_{j\in N_v} bd_j\right) - l_{0v}^t \tag{6}$$

For mobile precooling vehicles, their service capacity is formulated in a different way, as presented by Eq. (7). The term $S_a(i, R_c)$ in mobile precooling is equal to $S_b(i, R_c)$ minus order $i$'s service time.

$$S_b(i, R_c) = \min\left(t_0^l - l_{0v}^t, T_{max}\right) \tag{7}$$

Based on Eqs. (4) ∼ (6), it can be known that the developed evaluation function allows orders with lower insertion costs and smaller impacts on the vehicle's service capacity to be prioritized for insertion. Our preliminary numerical tests observed an average 2% improvement when employing the QTDD-based evaluation function compared to that not accounting for product quality.

For step (2) in repair heuristics, we consider the additional quality constraint and propose a customized insertion procedure for the repair heuristic in which new MP or CP routes are created after corresponding constraint checks, as shown in Fig. 7. When no feasible insertion positions can be found in the current solution, a new route needs to be constructed to include the current insertion node $i$. The constraint $C_s$ at the precooling service level is first checked (step 1). If $C_s$ is not respected after inserting node $i$, it means that the node cannot be inserted into a CP route. In this case, check the constraints at the MP route level (step 1.1), and if they are respected, create a MP route to serve node $i$. Note that if constraints at the MP route level in step 1.1 cannot be respected, it means that no feasible routes can be constructed to include node $i$, and then create a CP route to contain it and mark the current solution as an infeasible solution. If $C_s$ is respected after inserting node $i$ in step 1, check the constraints at the CP route level (step 2), and if the constraints are not respected, create a MP route to serve node $i$. If the constraints at the CP route level are respected in step 2, check the constraints at the MP route level (step 3), and if the constraints are not respected, create a CP route to serve node $i$. If the constraints at the MP route level are respected in step 3, it means that the node $i$ can be contained either in a CP route or a MP route. In this case, calculate the insertion cost of node $i$ in both a CP route and a MP route, and compare the results (step 3.1). If inseting node $i$ into a MP route causes few costs, create a MP route to serve node $i$; Otherwise, create a CP route to serve node $i$.

### 4.5. Improvement procedure

This study proposes a two-stage improvement procedure that is implemented at the end of the algorithm, aiming to further improve the solution quality by exchanging similar nodes. It is inspired from the classical removal heuristic proposed by Shaw (1997). This heuristic aims to remove node pairs that share similar attributes, in the hope of finding local improvement opportunities during the later repair procedure. In our procedure, we exchange similar nodes directly and test the improvement after each change. In this study, inter-service nodes are exchanged in the first stage, which is followed by the exchange among intra-service nodes.

The first-stage improvement procedure starts with determining the number of node pairs to be exchanged, which is followed by the determination of similar node pairs. In this study, four terms are used to calculate the similarity $S_{\mathrm{sim}\, i \in R_M, j \in R_C}(i, j)$ between nodes $i$ that belongs to MP route $R_M$ and node $j$ that belongs to CP route $R_C$, as shown in Eq. (8). The four terms reflect the QTDD attributes of orders including the initial product quality, the earliest service time, the volume of products, and the distance between two orders.

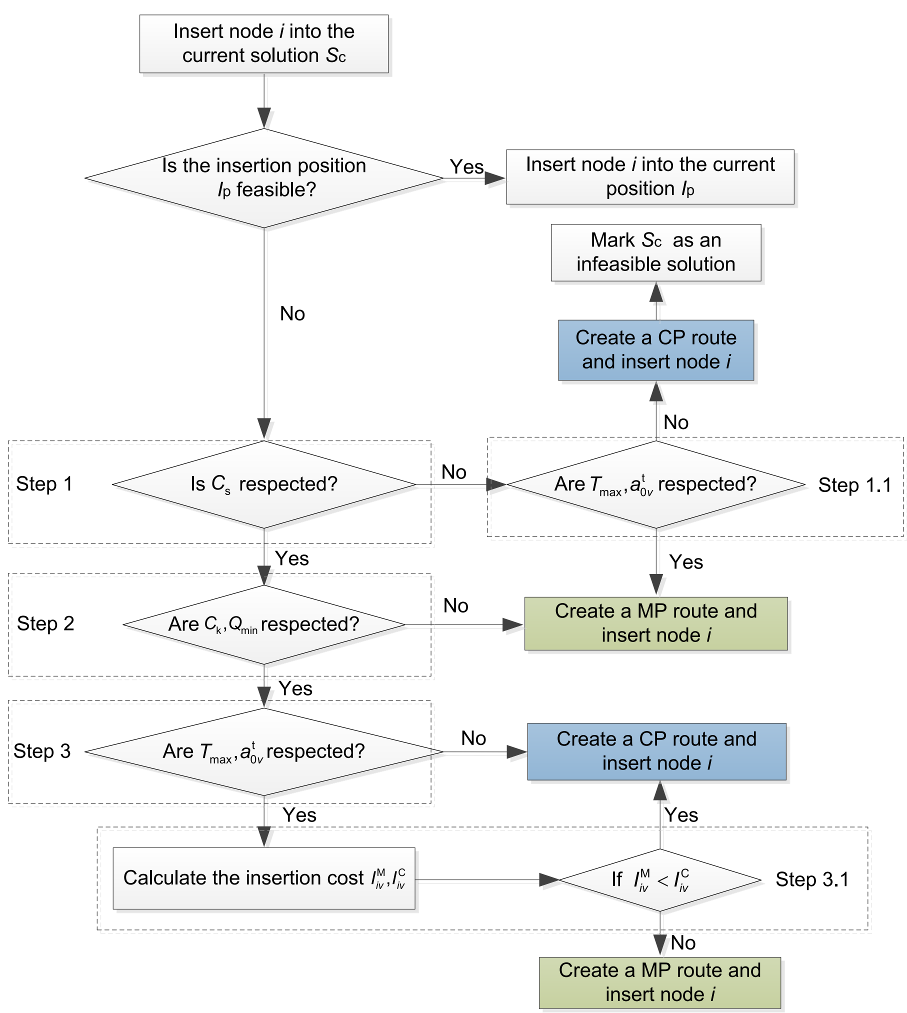


**Fig. 7.** The insertion procedure for the repair heuristics in the QTDD-based ALNS algorithm.

$$\underset{i\in R_{\mathrm{M}},j\in R_{\mathrm{C}}}{S_{\mathrm{sim}}}(i,j)=\xi_1\frac{\left|q_i^{\mathrm{ini}}-q_j^{\mathrm{ini}}\right|}{\max\limits_{i',j'\in F}\left|q_{i'}^{\mathrm{ini}}-q_{j'}^{\mathrm{ini}}\right|}+\xi_2\frac{\left|t_i^{\mathrm{e}}-t_j^{\mathrm{e}}\right|}{\max\limits_{i',j'\in F}\left|t_{i'}^{\mathrm{e}}-t_{j'}^{\mathrm{e}}\right|}+\xi_3\frac{\left|d_i-d_j\right|}{\max\limits_{i',j'\in F}\left|d_{i'}-d_{j'}\right|}+\xi_4\frac{d_{ij}}{\max\limits_{i',j'\in F}d_{i'j'}} \tag{8}$$

where $\xi_1, \xi_2, \xi_3, \xi_4$ denote the weights of the corresponding terms. Since time-related constraints are easy to be violated after exchanging nodes fulfilled by different services, related terms, such as $d_i$ and $t_i^e$ that affect the span of the service time and the start time of services, should keep similar as much as possible. Besides, a close distance between two nodes is necessary in finding the improvement. In this study, the values of $\xi_1$, $\xi_2, \xi_3, \xi_4$ are determined based on the adaptive adjustment mechanism used in Lin et al. (2023), during which the relationship $\xi_2, \xi_3 > \xi_4 > \xi_1$ is respected.

After the set of similar node pairs are determined, exchange node $i \in R_{\mathrm{M}}$ and the corresponding node $j \in R_{\mathrm{C}}$ on the copy of the current solution. Check the constraints $T_{\max}$, $a_{0v}^{\mathrm{t}}$, and $Q_{\min}$ of $R_{\mathrm{M}}$ and constraints $C_{\mathrm{s}}$, $C_{\mathrm{k}}$, $a_{0v}^{\mathrm{t}}$, and $Q_{\min}$ of $R_{\mathrm{C}}$. If all constraints are respected, calculate the exchange cost $E_{\mathrm{MC}}$ based on the sum of two insertion costs $C_{\mathrm{in}}(j, R_{\mathrm{M}})$ and $C_{\mathrm{in}}(i, R_{\mathrm{C}})$. If $E_{\mathrm{MC}} < 0$, exchange nodes $i$ and $j$ in the current solution. Here the way to calculate the insertion cost is the same as that in Lin et al. (2023).

Above steps repeat multiple iterations until no improvements are found in 100 iterations. The second-stage improvement procedure follows the similar framework with the first stage. However, in this stage, nodes from MP and CP routes are exchanged separately, in the hope of finding intra-service improvements. This directly affects the values of $\xi_1$, $\xi_2, \xi_3, \xi_4$ used in MP and CP. For MP services, high-quality levels of products are easy to be guaranteed, so the weight related to products' initial quality levels is set as a small value. Also, in CP services, considering the fact that the volume of orders has little impact on the span of the service time, the weight related to orders' demands is set as a small value. Similar to the first-stage improvement procedure, the values of $\xi_1, \xi_2, \xi_3, \xi_4$ in MP and CP are determined based on the adaptive adjustment mechanism, during which the relationships $\xi_1 < \xi_2, \xi_3, \xi_4$ and $\xi_3 < \xi_1, \xi_2, \xi_4$ are respected, respectively.

Based on the proposed improvement procedure, improvements ranging from 1% to 3% are observed during our preliminary tests based on multiple instances, reflecting the effectiveness of the proposed improvement procedure.

### 4.6. Implementation techniques

We use two techniques to reduce the time needed to calculate the product quality during the optimization procedure. First, considering the amount of time used by integral-formulation-based calculations, we discretize the quality decay function by dividing one hour into 100 segments and assume that the temperature and the corresponding decay rate in one segment is fixed, while guaranteeing the precision of the results. Second, based on the first technique, we construct a pre-processed quality matrix to calculate the product quality of individual farmers at any possible time in advance, avoiding having to conduct numerous quality evaluations during the execution of the optimization procedure. These implementation techniques significantly reduce the solving time of the optimization procedure. Detailed information on these techniques can be found in Appendix B.

## 5. Computational study

To illustrate the performance of the proposed vehicle routing model with the consideration of quality dynamics, we first apply the model in the case of sweet corn (Section 5.1). More specifically, in Section 5.1.1, we compare our model to the model that does not consider product quality and identify the underlying mechanism of achieving trade-offs between product quality and operating costs. In Section 5.1.2, we conduct temperature-related sensitivity analyses to evaluate the sensitivity of the model to different temperature profiles. In Section 5.2, we evaluate the performance of the proposed quality modeling approach within diverse scenarios and compare it with a simplified approach. To further test the performance of the proposed QTDD-ALNS algorithm in solving the proposed HFVRPTW-HFTQ model, in Section 5.3, we compare it with the CPLEX solver based on small-scale instances and three state-of-the-art algorithms based on large-scale instances. All tests were conducted on an Intel core i5-10210U 1.60GHz computer running Windows 10.

### 5.1. Applying the PQ model in decision-making: the case of sweet corn

#### 5.1.1. Impact of considering quality dynamics

Eighteen instances that are modified from Solomon VRPTW (vehicle routing problem with time window) instances are used in this section. We use clustered (C), random (R), and semi-random (RC) instances. C2, R2, and RC2 instances have wider time windows (2h) than C1, R1, and RC1 (1h) instances. The number 01 following C1, R1, RC1, C2, R2, and RC2 means that the percentage of customers with time windows is 100%. The number of nodes per cluster is either 25, 75, or 100, which comprise the final part of the label of an instance.

We choose sweet corn as an example and the decay rate function is set as $\alpha(T) = 0.0048e^{0.1036T}$, according to the data collected by Blackburn and Scudder (2009). The scheduling period is 6 hours from 6:00 am to 12:00 am. One hour is divided into 100 segments. Considering the fact that many regions have large daily temperature differences, we model the environment temperatures based on Eq. (9) leading to temperatures ranging from 15°C to 33°C between 0:00 am and 12:00 am. According to the results obtained by Lin et al. (2023) as well as our field study, the values of part of the parameters used in the model are set as follows: the maximum load capacity of collecting trucks is 2 tons; The maximum working duration of precooling vehicles is 6 hours; The precooling rate of mobile precooling vehicles is 18 min/100kg. Other parameters use the same values as those in Lin et al. (2023). Note that only the most efficient mobile precooling service (i.e., vacuum precooling) is used in the current study, we then use the same values to set the cost-related parameters of mobile precooling as those of vacuum precooling.

$$T(t) = \begin{cases} 15 & 0 \le t \le 600 \\ 3 * t/100 - 3 & 600 \le t \le 1200 \end{cases} \tag{9}$$

The proposed PQ model with the consideration of product quality was tested under the constraint of four different minimum quality levels (i.e., 93%, 92%, 91%, or 90%) to evaluate the performance. Note that different settings of the minimum quality levels may influence the absolute values of the result, but it will not influence the main conclusions drawn in this study. In addition, the model without considering product quality, which we refer to as the basic model, is also tested for comparison. Therefore, a total of 90 ($18 \times (4+1)$) scenarios is included in the experiment. Each scenario is run 10 times, and the average product quality of all orders, the minimum product quality of individual orders, and the total operating costs are recorded. Results are shown in Table 1.

In Table 1, the deviation values reflect the increase of the results obtained from the four PQ models (i.e., $\mathrm{Q}_{93\%}$, $\mathrm{Q}_{92\%}$, $\mathrm{Q}_{91\%}$, and $\mathrm{Q}_{90\%}$) compared to those from the basic model. Taking the deviation value in the Average product quality column as an example, $\mathrm{Dev}_{93\%}$ is calculated based on Eq. (10), where $Q_{93\%}^{\mathrm{ave-q}}$ and $\mathrm{Basic}_{\mathrm{ave-q}}$ denote the average product quality of orders calculated with the $\mathrm{Q}_{93\%}$ model and the basic model, respectively. The percentage is used as the unit for the basic model column for quality, indicating the levels of product quality when receiving precooling services. Also, RMB is utilized as the unit for total operating cost columns.

**Table 1**
Average and minimum product quality and total operating costs calculated with the basic model (without considering product quality as in Lin et al. (2023)) and the four PQ models (with the minimum quality level set to 93%, 92%, 91%, or 90%).

| Instances | Average product quality | | | | | Minimum product quality | | | | | Total operating cost | | | | |
|---|---|---|---|---|---|---|---|---|---|---|---|---|---|---|---|
| | Basic model (%) | Deviations from the basic model (%) | | | | Basic model (%) | Deviations from the basic model (%) | | | | Basic model (RMB) | Deviations from the basic model (%) | | | |
| | | $Dev_{93\%}$ | $Dev_{92\%}$ | $Dev_{91\%}$ | $Dev_{90\%}$ | | $Dev_{93\%}$ | $Dev_{92\%}$ | $Dev_{91\%}$ | $Dev_{90\%}$ | | $Dev_{93\%}$ | $Dev_{92\%}$ | $Dev_{91\%}$ | $Dev_{90\%}$ |
| C101_25 | 90.18 | 5.38 | 4.69 | 4.06 | 3.27 | 82.31 | 13.10 | 11.92 | 10.64 | 9.45 | 2187.10 | 24.30 | 14.18 | 9.56 | 2.63 |
| C201_25 | 87.08 | 10.00 | 8.77 | 7.95 | 7.09 | 75.71 | 23.04 | 21.64 | 20.24 | 18.91 | 2096.42 | 29.04 | 16.93 | 13.91 | 6.85 |
| R101_25 | 91.22 | 4.30 | 3.41 | 3.24 | 2.97 | 79.77 | 16.74 | 15.34 | 14.22 | 12.89 | 2808.83 | 20.56 | 13.56 | 12.45 | 11.95 |
| R201_25 | 89.54 | 6.82 | 5.70 | 5.27 | 4.04 | 82.18 | 13.29 | 11.96 | 10.79 | 9.61 | 2722.52 | 19.36 | 16.92 | 12.20 | 10.14 |
| RC101_25 | 90.09 | 5.65 | 5.35 | 4.73 | 4.48 | 80.01 | 16.30 | 15.15 | 13.89 | 12.57 | 3192.05 | 25.12 | 18.05 | 17.10 | 9.70 |
| RC201_25 | 89.03 | 7.22 | 6.40 | 5.45 | 4.43 | 79.68 | 16.78 | 15.52 | 14.27 | 12.99 | 2996.79 | 17.78 | 16.63 | 11.44 | 9.11 |
| C101_50 | 90.58 | 5.16 | 4.39 | 3.89 | 3.42 | 81.01 | 14.94 | 13.65 | 12.42 | 11.12 | 4716.88 | 31.97 | 22.53 | 16.82 | 11.50 |
| C201_50 | 89.87 | 5.86 | 5.17 | 3.97 | 3.99 | 77.00 | 20.86 | 19.52 | 18.34 | 16.97 | 4468.53 | 27.07 | 16.77 | 7.75 | 5.04 |
| R101_50 | 90.72 | 5.04 | 4.25 | 3.70 | 2.99 | 79.66 | 16.91 | 15.50 | 14.31 | 13.16 | 5147.47 | 32.62 | 22.84 | 17.74 | 11.79 |
| R201_50 | 90.21 | 5.37 | 4.83 | 4.27 | 3.11 | 81.17 | 14.64 | 13.47 | 12.14 | 10.92 | 5136.40 | 30.07 | 17.36 | 11.99 | 7.22 |
| RC101_50 | 90.50 | 5.02 | 4.69 | 4.06 | 3.73 | 77.30 | 20.35 | 19.15 | 17.77 | 16.51 | 5319.99 | 32.64 | 30.43 | 26.62 | 20.09 |
| RC201_50 | 89.85 | 5.81 | 5.48 | 4.51 | 4.23 | 80.37 | 15.80 | 14.59 | 13.39 | 12.08 | 5194.38 | 31.92 | 27.53 | 22.81 | 14.97 |
| C101_100 | 88.36 | 7.61 | 7.32 | 5.76 | 5.89 | 72.67 | 28.03 | 26.76 | 25.29 | 23.90 | 9110.89 | 64.72 | 54.46 | 38.73 | 29.95 |
| C201_100 | 90.01 | 6.41 | 5.05 | 4.33 | 3.57 | 81.03 | 14.80 | 13.69 | 12.33 | 11.21 | 9669.81 | 42.26 | 36.42 | 23.71 | 17.21 |
| R101_100 | 91.82 | 3.59 | 3.01 | 2.69 | 2.78 | 79.68 | 16.85 | 15.50 | 14.36 | 13.06 | 9961.09 | 27.52 | 22.44 | 13.63 | 12.61 |
| R201_100 | 91.92 | 3.69 | 2.72 | 2.19 | 1.38 | 78.31 | 18.77 | 17.51 | 16.36 | 14.97 | 9754.64 | 31.24 | 14.29 | 15.04 | 8.65 |
| RC101_100 | 89.48 | 6.57 | 5.35 | 5.62 | 4.81 | 78.64 | 18.34 | 17.13 | 15.78 | 14.48 | 9844.50 | 34.91 | 32.33 | 26.20 | 19.73 |
| RC201_100 | 91.63 | 4.45 | 3.26 | 2.39 | 1.75 | 85.97 | 8.22 | 7.11 | 5.87 | 4.84 | 10093.16 | 28.53 | 21.43 | 15.58 | 10.07 |
| Ave | | **5.77** | **4.99** | **4.34** | **3.77** | | **17.10** | **15.84** | **14.58** | **13.31** | | **30.51** | **22.58** | **17.40** | **12.18** |

$$\mathrm{Dev}_{93\%} = \left(Q_{93\%}^{\mathrm{ave\_q}} - \mathrm{Basic}_{\mathrm{ave\_q}}\right) / \mathrm{Basic}_{\mathrm{ave\_q}} * 100\% \tag{10}$$

It can be seen from Table 1 that compared to the PQ model, without considering the minimum quality level constraint, the operating cost is reduced but the average product quality and the minimum product quality are lower. Compared to the basic model, considering a 93% minimum quality level, the operating cost increases by an average of 30.51%, and the average product quality as well as the minimum product quality increase by an average of 5.77% and 17.10%, respectively. Here the ratio of 30.51% and 5.77% is 5.29, meaning that for every 1% improvement in average product quality, the operating cost needs to be increased by 5.29%. We call this ratio as CQ ratio. When the minimum quality level decreases to 92%, 91%, and 90%, the CQ ratio decreases to 4.53, 4.01, and 3.23, respectively. As can be seen from Table 1, the improvement of the minimum product quality is significant, which helps to reduce the product quality differences among farmers. In addition, it is found that for the basic model, the average product quality of all orders decreases in most instances when the time windows are wider, while that does not happen for the PQ model. Due to the constraint of the minimum quality level, the minimum product quality of individual orders for the PQ model is guaranteed to be a high level, while for the basic model, that can decrease to relatively low levels. Moreover, it is noticed that for both the PQ model and the basic model, in most cases, the operating cost is reduced when orders' time windows become wider.

Taking instance C101_100 as an example, Fig. 8 shows the best vehicle routing solutions obtained from the basic model and the PQ model under the minimum quality levels of 90%, 91%, 92%, and 93%, respectively. Here green and bule lines depict the vehicle routes of MP and CP, respectively. As can be seen from Fig. 8 (a), CP dominates MP in the basic model and the $Q_{90\%}$ model. With the increase of the minimum quality level, the use of MP increase, which is because the timely service of MP contributes to less quality losses.

To identify the underlying mechanism that can further explain the performance of the proposed PQ model, we compare the performance of MP and CP based on the best solutions obtained for each of the 18 instances. Fig. 9 illustrates the range of the average demand $d_i$, the average distance to the station $d_{0i}$, the average initial product quality $q_i^{\mathrm{ini}}$, and the average earliest service time $t_i^{\mathrm{e}}$ of the orders served by MP and CP in all 18 instances. As can be seen from Fig. 9 (a) and Fig. 9 (b), in the basic model and the two PQ models, MP tends to serve the smaller-volume orders, and CP tends to serve orders that are closer to the precooling station. The former is due to the limited precooling speed of MP, while the latter is because of the relatively high travel costs of CP. In addition, as shown in Fig. 9 (c) and Fig. 9 (d), in the two PQ models rather than the basic model, CP tends to serve orders which have higher $q_i^{\mathrm{ini}}$ or earlier $t_i^{\mathrm{e}}$. This is because CP causes more quality losses than MP during the service, and then CP is more likely to serve orders with high initial product quality and earlier earliest service time (the earlier $t_i^{\mathrm{e}}$, the low temperatures). The above results show that MP and CP are complementary to each other in terms of fulfilling requests in the PQ model.

The above findings indicate that adjusting $Q_{\min}$ values plays a crucial role in achieving trade-offs between product quality and operational costs, where higher $Q_{\min}$ values lead to improved product quality but increased operating costs. Also, wider time windows result in reduced operating costs while still satisfying the minimum quality level ($Q_{\min}$) constraint within our model. The basic model that does not account for product quality provides a benchmark for the best operating cost results with the worst product quality results. It should be noted that tweaking time windows within our benchmark model affects both operating costs and product quality due to the absence of the minimum quality level constraint; thus reducing operating costs comes at the expense of decreased product quality.

### 5.1.2. *Effect of different temperature profiles*

Considering the impact of the temperature on product quality, this

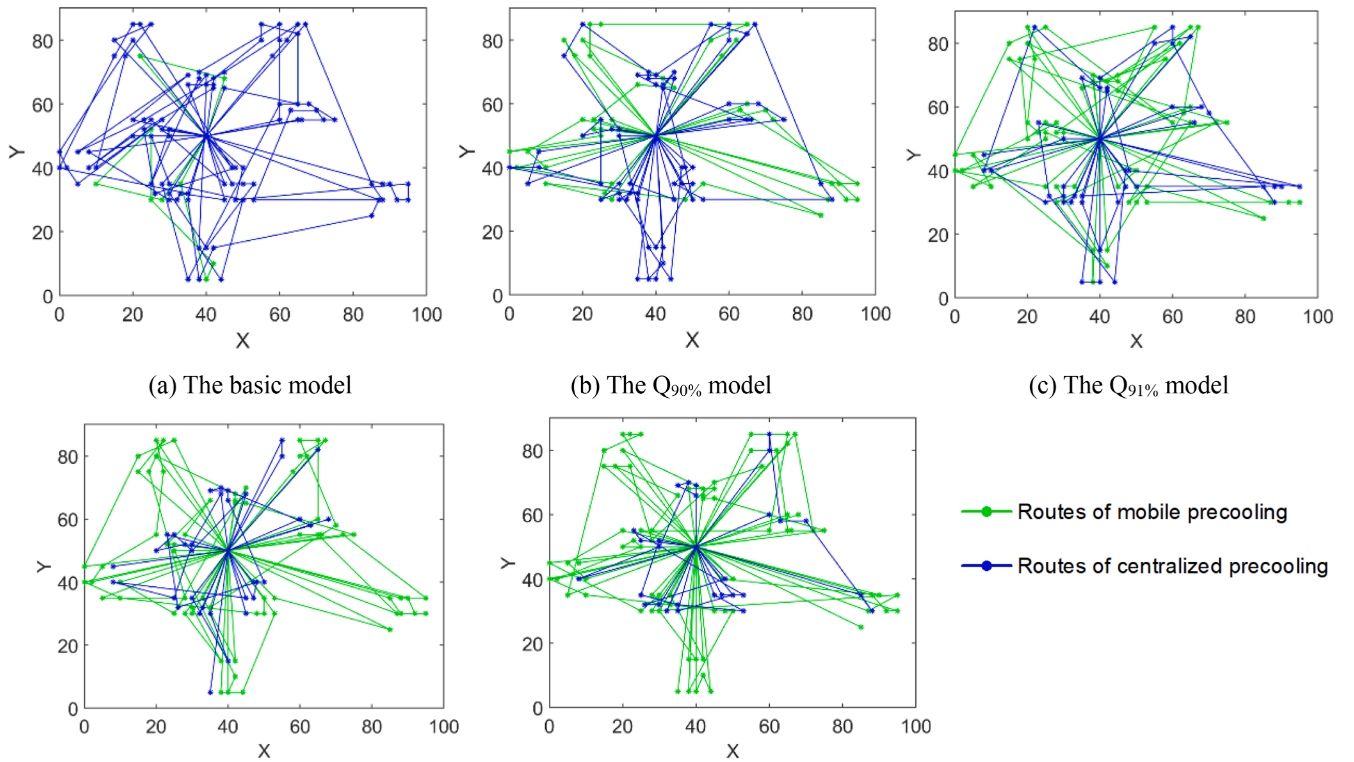


(a) The basic model (b) The $Q_{90\%}$ model (c) The $Q_{91\%}$ model

(d) The $Q_{92\%}$ model (e) The $Q_{93\%}$ model

**Fig. 8.** Best vehicle routes calculated with the basic model (a) (without considering product quality as in Lin et al. (2023)) and the PQ model (with the minimum quality level constraint) applied to four different quality levels (b, c, d and e).

section aims to evaluate the sensitivity of the calculated solutions to different temperature levels. Here we consider the scenarios of low temperatures and high temperatures, as shown in Fig. 10. The minimum quality level is set to the value that increases the operating cost by around 10% compared to the basic model. For the scenario of original temperatures, we chose the results of the $Q_{90\%}$ model in Section 5.1.1 for comparison. Tests are based on the above 18 instances, and each of them is run 10 times. The average product quality of all orders, the minimum product quality of individual orders, and total operating costs obtained from both the basic model and PQ models are recorded. Results are shown in Table 2, where the deviation values reflect the increase (for positive values) and the decrease (for negative values) of the results obtained from PQ models compared to those from the basic model.

In original tests, considering a 90% minimum quality level, the CQ ratio is equal to 3.23. In the scenario of low temperatures, as shown in Table 2, the CQ ratio equals 5.55, reflecting that it costs much for 1% product quality improvement. When the temperature is high, the total operating cost increases by an average of 9.91%, and the average product quality as well as the minimum product quality increase by an average of 7.66% and 26.50%, respectively. In this case, the CQ ratio equals 1.29, which is significantly lower than that in the low-temperature scenario. The above results prove the high sensitivities of the PQ model to temperature settings and also verify the effectiveness of the proposed model in improving product quality especially when the environment temperature is relatively high.

### *5.2. Impacts of quality decay functions on scheduling results*

This section aims to investigate the effects of different quality decay functions on the scheduling outcomes of the PQ problem. The proposed quality decay function, which is based on time-varying temperatures, is compared with a simplified function that utilizes average temperatures. Nine instances are generated with varying picking periods, length of time windows, temperatures during the scheduling period, minimum quality levels, and decay rates. Table 3 presents the scenario settings for the tested instances. The temperature function in instances 1 to 6 is derived from Eq. (12), while in instances 7 to 9 it is based on Eq. (13). Each of the nine instances consists of 12 orders, and parameters used in the mathematical model are set to identical values as those in Section 5.1.1.

$$T(t) = \begin{cases} 25 & 0 \le t \le 600 \\ 2 * t/100 + 13 & 600 \le t \le 1200 \end{cases} \tag{12}$$

$$T(t) = \begin{cases} 15 & 0 \le t \le 600 \\ t/100 + 9 & 600 \le t \le 1200 \end{cases} \tag{13}$$

The two quality decay functions mentioned above are applied to the PQ model. Each instance is run 10 times using the proposed ALNS algorithm, and the minimum operating cost and average product quality of all orders are recorded. Results are presented in Table 4, with columns Cost Dev and Quality Dev indicating the deviation of results obtained from the simplified quality decay function (referred to as Method 2) compared to the proposed function (referred to as Method 1).

As shown in Table 4, the utilization of the simplified quality decay function leads to an enhancement in the average quality of orders; however, it also results in a substantial increase in operating costs across eight instances. This is attributed to the inability of average temperatures as inputs to accurately represent the actual product quality decay process. Specifically, during the tested instances, Method 2 causes an underestimation of product quality followed by tighter time window constraints (please refer to Appendix C for further details), ultimately leading to higher costs and improved product quality. Notably, for instance 9, two different quality decay functions yield identical outcomes due to slow product deterioration at low temperatures and a low minimum quality level. Consequently, decisions related to quality have

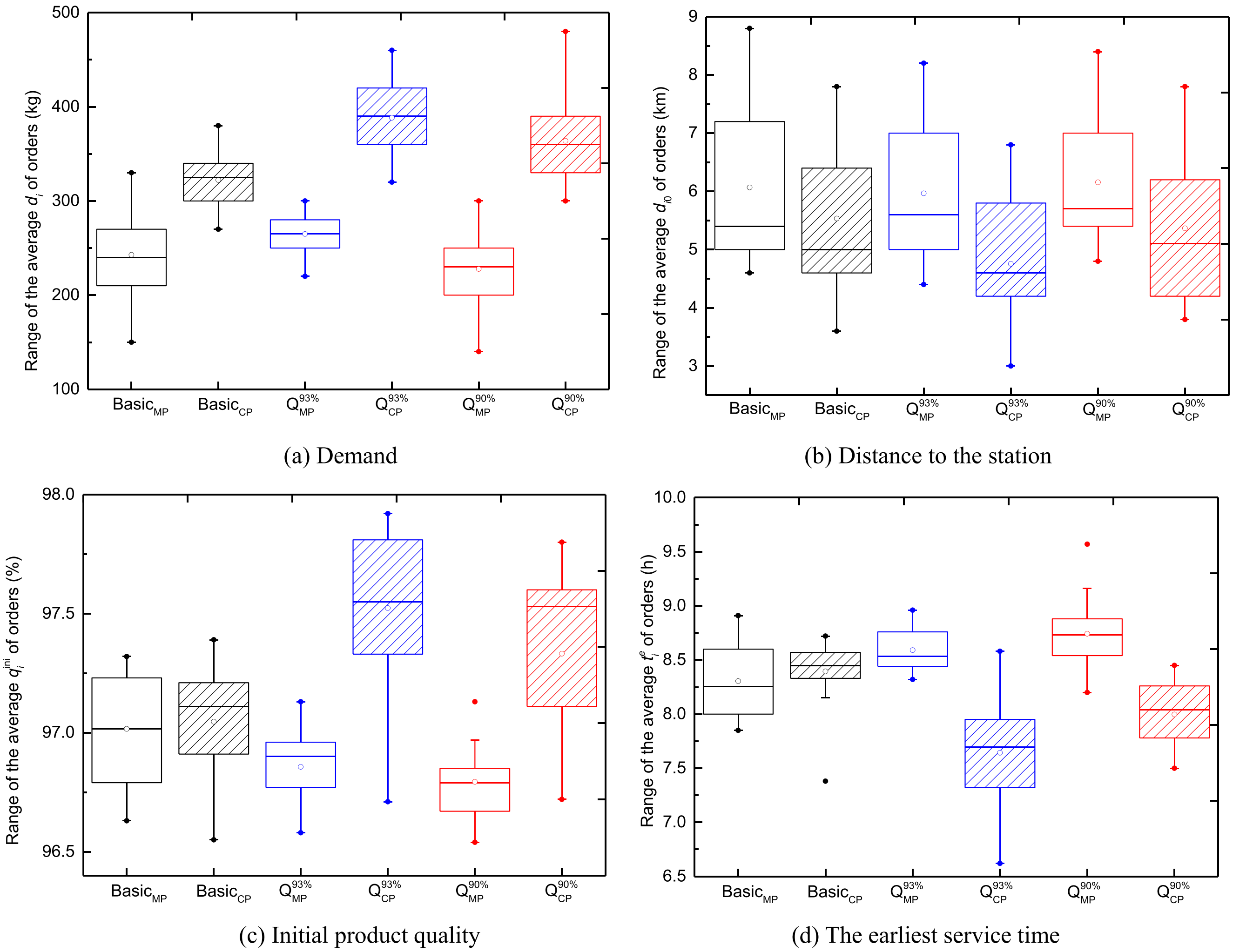


**Fig. 9.** The complementarity of mobile precooling and centralized precooling in fulfilling orders in the basic model (without considering product quality as in Lin et al. (2023)) and two PQ models (with the minimum quality level constraint). Figure (a) illustrates the average demands of orders served by mobile precooling and centralized precooling, while figures (b), (c), and (d) present the results for the average distance to the station, average initial product quality, and average earliest service times of orders.

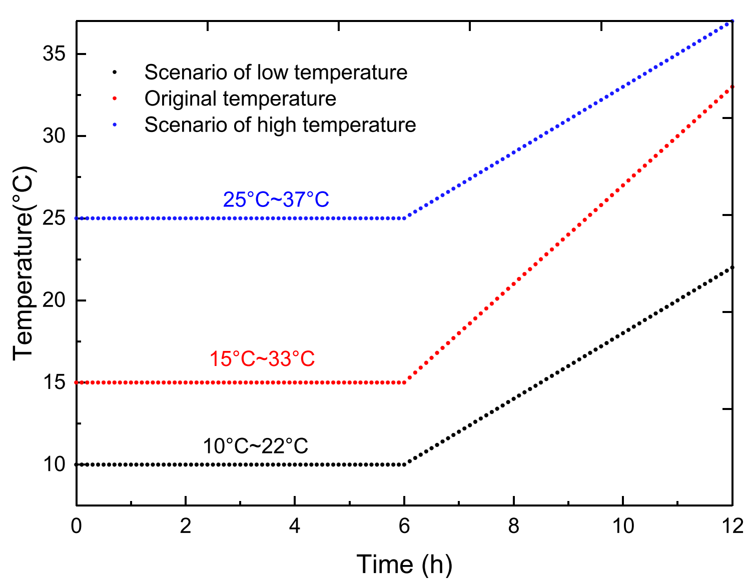


**Fig. 10.** Assumed temperature change with time in the sensitivity tests.

**Table 2**
Average and minimum product quality and total operating costs calculated with the basic model (without considering product quality as in Lin et al. (2023)) and the PQ model in different temperatures profiles (In the tested low temperature and high temperature scenarios, the minimum quality levels in the PQ model are set to 95% and 80%).

| Instances | Low temperatures | | | | | | High temperatures | | | | | |
|---|---|---|---|---|---|---|---|---|---|---|---|---|
| | Basic model | | | Deviations from the basic model (%) | | | Basic model | | | Deviations from the basic model (%) | | |
| | Average product quality (%) | Minimum product quality (%) | Total operating cost (RMB) | $Dev_{Ave\_Q}$ | $Dev_{Min\_Q}$ | $Dev_{Tot\_C}$ | Average product quality (%) | Minimum product quality (%) | Total operating cost (RMB) | $Dev_{Ave\_Q}$ | $Dev_{Min\_Q}$ | $Dev_{Tot\_C}$ |
| C101_25 | 94.54 | 89.16 | 2187.10 | 2.21 | 6.61 | 4.40 | 85.42 | 68.67 | 2187.10 | 0.96 | 16.63 | 5.14 |
| C201_25 | 94.12 | 89.42 | 2096.42 | 2.75 | 6.27 | 7.44 | 75.64 | 58.95 | 2096.42 | 13.50 | 35.86 | 8.70 |
| R101_25 | 96.08 | 91.30 | 2808.83 | 1.16 | 4.33 | 10.98 | 83.30 | 65.05 | 2808.83 | 7.12 | 23.18 | 11.95 |
| R201_25 | 95.33 | 92.51 | 2722.52 | 1.28 | 2.86 | 7.21 | 80.19 | 69.23 | 2722.52 | 8.64 | 16.34 | 10.04 |
| RC101_25 | 96.85 | 93.41 | 3192.05 | 0.02 | 1.85 | 3.64 | 86.17 | 72.53 | 3192.05 | 1.38 | 10.92 | 8.31 |
| RC201_25 | 95.03 | 90.29 | 2996.79 | 2.03 | 5.36 | 5.48 | 79.00 | 61.70 | 2996.79 | 9.99 | 30.66 | 9.60 |
| C101_50 | 95.76 | 91.80 | 4716.88 | 0.91 | 3.62 | 1.05 | 81.77 | 66.74 | 4716.88 | 5.82 | 20.08 | 6.16 |
| C201_50 | 95.40 | 89.93 | 4468.53 | 1.31 | 5.76 | 1.41 | 80.40 | 60.58 | 4468.53 | 6.84 | 32.47 | 4.44 |
| R101_50 | 95.78 | 91.52 | 5147.47 | 1.09 | 3.86 | 7.37 | 81.84 | 65.79 | 5147.47 | 7.27 | 22.16 | 13.59 |
| R201_50 | 95.53 | 92.11 | 5136.40 | 0.98 | 3.30 | 2.83 | 80.83 | 67.83 | 5136.40 | 6.99 | 18.33 | 5.33 |
| RC101_50 | 95.80 | 90.47 | 5319.99 | 1.10 | 5.06 | 13.65 | 82.05 | 62.32 | 5319.99 | 5.12 | 28.45 | 14.72 |
| RC201_50 | 95.41 | 91.54 | 5194.38 | 1.05 | 3.97 | 11.15 | 80.37 | 65.72 | 5194.38 | 7.58 | 22.31 | 14.10 |
| C101_100 | 94.87 | 88.49 | 9110.89 | 1.74 | 7.50 | 18.54 | 78.33 | 56.14 | 9110.89 | 8.99 | 42.66 | 21.73 |
| C201_100 | 95.50 | 91.56 | 9669.81 | 0.79 | 3.99 | 3.01 | 66.21 | 39.93 | 9669.81 | 29.71 | 100.70 | 11.80 |
| R101_100 | 96.31 | 93.20 | 9961.09 | 0.26 | 2.24 | 2.03 | 83.96 | 71.71 | 9961.09 | 2.67 | 11.76 | 5.93 |
| R201_100 | 96.26 | 93.36 | 9754.64 | 0.24 | 1.97 | 2.58 | 83.47 | 72.28 | 9754.64 | 2.86 | 11.00 | 4.96 |
| RC101_100 | 95.35 | 90.85 | 9844.50 | 1.63 | 4.77 | 9.49 | 80.23 | 64.34 | 9844.50 | 8.64 | 24.70 | 15.26 |
| RC201_100 | 96.10 | 93.68 | 10093.16 | 0.46 | 1.42 | 4.55 | 83.05 | 73.51 | 10093.16 | 3.84 | 8.86 | 6.58 |
| Ave | | | | **1.17** | **4.15** | 6.49 | | | | **7.66** | **26.50** | **9.91** |

**Table 3**
Scenario settings in the tested instances.

| Instances | Orders' average picking periods | Length of orders' time windows | Temperature ranges | Minimum quality levels | Decay rate function |
|---|---|---|---|---|---|
| 1 | 2h | 1h | 25°C~37°C | 80% | $\alpha(T) = 0.0048e^{0.1036T}$ |
| 2 | 2h | 1h | 25°C~37°C | 75% | |
| 3 | 2h | 2h | 25°C~37°C | 75% | |
| 4 | 2h | 2h | 25°C~37°C | 80% | |
| 5 | 1h | 1h | 25°C~37°C | 85% | |
| 6 | 1h | 1h | 25°C~37°C | 80% | |
| 7 | 2h | 1h | 15°C~21°C | 90% | |
| 8 | 2h | 1h | 15°C~21°C | 85% | |
| 9 | 2h | 1h | 15°C~21°C | 80% | |

**Table 4**
Results of the PQ instances under two quality decay functions.

| Instances | Method 1 (Using average temperatures) | | Method 2 (Using time-varying temperatures) | | Cost Dev | Quality Dev |
|---|---|---|---|---|---|---|
| | Cost | Average quality | Cost | Average quality | | |
| 1 | 1466.88 | 85.26% | 1971.64 | 87.87% | 34.41% | 3.06% |
| 2 | 1466.88 | 85.26% | 1716.18 | 86.65% | 17.00% | 1.63% |
| 3 | 1466.88 | 85.26% | 1583.78 | 86.20% | 7.97% | 1.10% |
| 4 | 1466.88 | 85.26% | 2007.44 | 87.67% | 36.85% | 2.83% |
| 5 | 1659.80 | 89.62% | 2007.44 | 91.37% | 20.94% | 1.95% |
| 6 | 1466.88 | 88.89% | 1584.87 | 90.47% | 8.04% | 1.78% |
| 7 | 1429.18 | 94.32% | 1691.58 | 94.98% | 18.36% | 0.70% |
| 8 | 1252.12 | 92.99% | 1422.84 | 93.77% | 13.63% | 0.84% |
| 9 | 1252.12 | 92.99% | 1252.12 | 92.99% | 0.00% | 0.00% |

no impact on scheduling results.

The aforementioned findings suggest that the utilization of a simplistic product quality decay function may lead to significant divergence from actual scheduling outcomes, thereby verifying the effectiveness and significance of employing time-varying temperatures to accurately represent the product quality decay process.

### 5.3. *Effectiveness of the proposed QTDD-based ALNS algorithm*

#### 5.3.1. *Small-scale instances*

In this section, we test the performance of the proposed QTDD-based ALNS algorithm based on small-scale PQ instances and compare the results with the results of the CPLEX solver. Since CPLEX cannot deal with the nonlinear constraint Eq. (1), we use a linear function to replace the proposed nonlinear function of quality decay, which is specifically tailored to closely approximate the curve of the nonlinear function for an effective representation of the nonlinear constraint. The number of orders ranges from 10 to 17. Instances are tested under three different minimum quality levels. The QTDD-algorithm solves each instance 10 times, and the best solutions as well as the average solving time are recorded. The maximum solving time of CPLEX is set to 10800 seconds. Results are shown in Table 5.

As can be seen from Table 5, the proposed QTDD-based ALNS algorithm can solve the instances to optimality when the number of orders is below 14. With the increase of the order's number, the proposed QTDD-algorithm can only obtain optimal solutions under part of minimum quality levels. For those instances, the average optimality gap is around 1%, as depicted in column $Ave_{opt\_gap}$. When the number of orders is equal to 17, CPLEX could not obtain optimal solutions within 3 hours, while the average solution time of our QTDD-based ALNS algorithm is no more than 1 minute.

**Table 5**
Best results calculated with CPLEX and the QTDD-based ALNS algorithm on solving small-scale instances (the number of nodes ranges from 10 to 17).

| Instances | CPLEX | | | | | | QTDD-based ALNS | | | | | | $Ave_{opt\_gap}$ (%) |
|---|---|---|---|---|---|---|---|---|---|---|---|---|---|
| | Q1 | | Q2 | | Q3 | | Q1 | | Q2 | | Q3 | | |
| | $C_{opt}$ | Time (s) | $C_{opt}$ | Time (s) | $C_{opt}$ | Time (s) | $C_{best}$ | Time (s) | $C_{best}$ | Time (s) | $C_{best}$ | Time (s) | |
| R101_10 | 1399.10 | 22.75 | 1323.86 | 23.39 | 1282.84 | 24.54 | **1399.10** | 11.10 | **1323.86** | 12.78 | **1282.84** | 16.13 | **0.00** |
| R101_11 | 1536.16 | 32.85 | 1395.28 | 34.32 | 1392.09 | 42.29 | **1536.16** | 18.53 | **1395.28** | 14.51 | **1392.09** | 13.54 | **0.00** |
| R101_12 | 1547.33 | 40.83 | 1405.61 | 36.78 | 1403.26 | 63.78 | **1547.33** | 18.75 | **1405.61** | 20.24 | **1403.26** | 14.46 | **0.00** |
| R101_13 | 1636.41 | 49.83 | 1499.27 | 82.73 | 1477.64 | 103.27 | **1636.41** | 20.18 | **1499.27** | 19.16 | **1477.64** | 19.97 | **0.00** |
| R101_14 | 1915.77 | 1288.50 | 1634.89 | 182.36 | 1530.05 | 243.77 | **1915.77** | 27.49 | **1634.89** | 25.35 | 1596.13 | 20.94 | 1.44 |
| R101_15 | 2005.56 | 499.58 | 1773.16 | 277.62 | 1690.25 | 2725.02 | 2014.45 | 27.63 | 1776.28 | 26.92 | **1690.25** | 23.42 | 0.21 |
| R101_16 | 2044.04 | 4784.97 | 1830.13 | 2354.03 | 1728.72 | 3450.88 | 2047.49 | 31.28 | 1833.25 | 33.28 | **1728.72** | 41.30 | 0.11 |
| R101_17 | —— | —— | —— | | —— | | 2128.12 | 35.72 | 1958.14 | 37.23 | 1926.20 | 45.91 | —— |
| Ave time | | 959.90 | | 427.32 | | 950.51 | | 22.14 | | 21.75 | | 21.39 | |

Note: Q1=95%, Q2=94%, Q3=93%. $C_{opt}$ denotes the optimal solution solved by CPLEX in 3 hours. $C_{best}$ denotes the best solution solved by QTDD-based ALNS in 10 runs. Column Ave dev shows the average deviations of the obtained best solutions from the optimal solutions.

### 5.3.2. *Large-scale instances*

As shown in Section 5.3.1, CPLEX could not solve large-scale PQ instances with 17 orders to optimality. Also, existing algorithms are not available for solving the studied problem. We therefore test the performance of the QTDD-based ALNS algorithm for solving large-scale instances based on instances of closely related problems: HFVRPTW. We slightly modified our algorithm to solve 24 HFVRPTW benchmark instances with 100 nodes proposed by Koc et al. (2015). Three state-of-the-art algorithms are chosen for horizontal comparison, including the HEA algorithm proposed by Koc et al. (2015), the BAC algorithm presented by Fachini and Armentano (2020), and the classic ALNS algorithm proposed by Lin et al. (2023). Table 6 provides a summary of the aforementioned three algorithms, accompanied by a concise description of their primary contexts.

The QTDD-based ALNS algorithm solves each instance 10 times, and the best solutions and the average solutions are reported. Results are shown in Table D1 in Appendix D, where the average solving time of the QTDD-based ALNS algorithm reflects the average time across ten runs that no improved solutions are obtained in 100 generations.

**Table 6**
Algorithms used in the large-scale instances testing.

| Acronym | Full name | Reference | Primary contexts |
|---|---|---|---|
| HEA | Hybrid evolutionary algorithm | Koc et al. (2015) | The algorithm integrates adaptive large neighborhood search into an evolutionary algorithm, utilizing ALNS for generating the initial population and optimizing offspring, while incorporating an improved splitting procedure to handle infeasibilities. |
| BAC | Branch-and-check | Fachini and Armentano (2020) | The algorithm decomposes the HFVRPTW problem into a generalized assignment master problem and independent traveling salesman subproblems with time windows. Valid optimality and feasibility cuts are devised to ensure the convergence of the algorithms. |
| ALNS | Adaptive large neighborhood search | Lin et al. (2023) | The algorithm contains a multi-level struct-based solution representation, based on which customized solution evaluations, feasibility checks as well as neighborhood search heuristics are developed. |

As shown in Table D1, the proposed QTDD-based ALNS algorithm is quite competitive compared to the three existing algorithms. In terms of solution quality, the average deviations to HEA, BAC, and ALNS are 0.88%, -1.22%, and -1.06%, respectively. This suggests that the proposed QTDD-based ALNS algorithm is slightly inferior to HEA and superior to BAC and the classic ALNS with regards to the HFVRPTW instances. In terms of solution times, both our algorithm and the HEA algorithm are efficient with the average solving time no more than 6 minutes.

## 7. Discussion and conclusions

This study focuses on modeling product quality dynamics in the optimization of post-harvest transport operations, aiming to provide insights into reducing the quality losses of highly perishable products before they enter temperature-controlled supply chains. Traditional centralized precooling and emerging mobile precooling are concurrently applied to fulfill a series of small-scale and scattered precooling requests, with the goal of minimizing the total operating cost while guaranteeing product quality for farmers. We develop a new integral formulation for modeling dynamic temperature-dependent product quality decay and integrate it into a vehicle routing model as a constraint. A QTDD-based ALNS algorithm is designed to solve the model, which leverages the complementary nature of facilities' service capabilities for order fulfillment. To reduce the time needed to calculate the product quality during the optimization procedure, we discretize the integral function and introduce a quality matrix to store the product quality for individual orders at any possible time in advance. Results based on both small-scale instances and large-scale instances show the effectiveness and efficiency of the QTDD-based ALNS algorithm by comparing it with CPLEX solver and three state-of-the-art algorithms. Furthermore, we find that considering product quality decay in the vehicle routing model does not increase the solving time substantially, which is mainly because of our QTDD strategy and the quality-matrix-based implementation techniques. We also demonstrate that having more detailed temperature data in modeling product quality deterioration might result in more accurate decisions with economic and quality gains, compared to a simplified quality modeling method that simply uses average temperature data.

We compare the results of the current model with the model by Lin et al. (2023), which does not consider product quality decay. We show that the former contributes to improving the average product quality of all orders as well as the minimum product quality of individual orders, while it increases the total operating cost, due to the inherent trade-off between product quality and costs. It is verified that considering product quality is more cost-efficient when the temperatures are higher. Moreover, our model guarantees the minimum quality level of orders, which helps to achieve a relatively fair service and reduces farmers' dissatisfaction due to the differences in the quality levels among farmers.

The minimum quality level plays an important role in achieving trade-offs between product quality and operational costs. The higher the minimum quality level, the higher the total operating cost, which further affects the decisions of stakeholders. For instance, service providers can price different-level precooling services based on the cost under certain minimum quality level. Smallholder farmers can also decide which level of the precooling service to choose according to the market price of products to maximize benefits. This becomes applicable with the current fast development of information technologies that enable the traceability of product quality from production to consumption (see e.g., Yang et al., 2022; Yang et al., 2023). In addition to the minimum quality level, the length of precooling orders' time windows can significantly influence the results. We find that wider time windows of precooling orders can help to reduce the total operating cost, which confirms the results in Lin et al. (2023). At the same time, for the model that does not consider product quality, wider time windows often lead to lower quality levels of orders, while that does not happen for our model because of the minimum quality level constraint. We therefore suggest service providers to offer farmers wider service time slots when applying the model to save the total operating cost without reducing product quality.

In conclusion, our study quantifies the advantages of managing product quality in the early stage of supply chains for perishable products and provides management insights on conducting quality-based precooling services. We also verify the key role of temperatures in capturing the dynamic nature of product quality, which further proves the significance of considering temperature-dependent product quality decay for the transportation and distribution of perishable products.

## CRediT authorship contribution statement

**Na Lin:** Writing – original draft, Software, Methodology, Investigation, Data curation, Conceptualization. **Argyris Kanellopoulos:** Writing – review & editing, Supervision, Conceptualization. **Renzo Akkerman:** Writing – review & editing, Supervision, Conceptualization. **Jianghua Zhang:** Supervision, Project administration, Conceptualization. **Junhu Ruan:** Supervision, Project administration, Conceptualization.

## Acknowledgments

This work was supported by the National Social Science Foundation of China [grant number 22&ZD151].

## Appendix A

$$\min Z_1 + Z_2 + Z_3 + Z_4 \tag{A.1}$$

$$Z_1 = \sum_{j\in F}\sum_{v\in V}\sum_{o=1} x^o_{0jv} h_\mathrm{p} + \sum_{j\in F}\sum_{v\in V}\sum_{o=2} x^o_{0jv}(h_\mathrm{k} + h_\mathrm{r}) \tag{A.2}$$

$$Z_2 = \sum_{i\in F\cup 0}\sum_{j\in F\cup 0, j\neq i}\sum_{v\in V}\sum_{o=1} x^o_{ijv} d_{ij} f_\mathrm{p} + \sum_{i\in F\cup 0}\sum_{j\in F\cup 0, j\neq i}\sum_{v\in V}\sum_{o=2} x^o_{ijv} d_{ij}(f_\mathrm{k} + f_\mathrm{r}) \tag{A.3}$$

$$Z_3 = \sum_{i\in F}\sum_{j\in F\cup 0, j\neq i}\sum_{v\in V}\sum_{o=1} x^o_{ijv} d_i u_\mathrm{p} + \sum_{i\in F}\sum_{j\in F\cup 0, j\neq i}\sum_{v\in V}\sum_{o=2} x^o_{ijv} d_i u_\mathrm{s} \tag{A.4}$$

$$Z_4 = \sum_{i\in F}\sum_{v\in V}\left(\varphi_1 m^\mathrm{t}_{iv} + \varphi_2 n^\mathrm{t}_{iv}\right) \tag{A.5}$$

$$s.t. \sum_{i\in F\cup 0, i\neq j}\sum_{v\in V}\sum_{o\in O} x^o_{ijv} = 1 \qquad \forall j \in F \tag{A.6}$$

$$\sum_{j\in F}\sum_{o\in O} x^o_{0jv} \leq 1 \qquad \forall v \in V \tag{A.7}$$

$$\sum_{i\in F\cup 0, i\neq j} x^o_{ijv} - \sum_{i\in F\cup 0, i\neq j} x^o_{jiv} = 0 \qquad \forall j \in F\cup 0, \forall v \in V, \forall o \in O \tag{A.8}$$

$$\sum_{i\in F}\sum_{j\in F\cup 0, j\neq i}\sum_{o=2} x^o_{ijv} d_i \leq C_\mathrm{k} \qquad \forall v \in V \tag{A.9}$$

$$\sum_{i\in F}\sum_{j\in F\cup 0, j\neq i}\sum_{v\in V}\sum_{o=2} x^o_{ijv} d_i \leq C_\mathrm{s} \tag{A.10}$$

$$T_{\max} \geq a^\mathrm{t}_{0v} - l^\mathrm{t}_{0v} - M_\mathrm{T}\left(1 - \sum_{j\in F}\sum_{o=1} x^o_{0jv}\right) \qquad \forall v \in V \tag{A.11}$$

$$l^\mathrm{t}_{0v} \geq t^\mathrm{e}_i - t_{0i} - M_\mathrm{T}\left(1 - \sum_{o\in O} x^o_{0iv}\right) \qquad \forall i \in F, \forall v \in V \tag{A.12}$$

$$a^\mathrm{t}_{jv} \geq a^\mathrm{t}_{iv} + m^\mathrm{t}_{iv} + q^\mathrm{t}_{iv} + t_{ij} - M_\mathrm{T}\left(1 - \sum_{o\in O} x^o_{ijv}\right) \qquad \forall i \in F, j \in F\cup 0, j \neq i, \forall v \in V \tag{A.13}$$

$$m^\mathrm{t}_{iv} \geq t^\mathrm{e}_i - a^\mathrm{t}_{iv} - M_\mathrm{T}\left(1 - \sum_{j\in F\cup 0, j\neq i}\sum_{o\in O} x^o_{ijv}\right) \qquad \forall i \in F, \forall v \in V \tag{A.14}$$

$$n_{iv}^{t} \geq a_{iv}^{t} - t_{i}^{l} - M_{T}\left(1 - \sum_{j \in F \cup 0, j \neq i} \sum_{o \in O} x_{ijv}^{o}\right) \qquad \forall i \in F, \forall v \in V \tag{A.15}$$

$$q_{iv}^{t} \geq (2b + r_{p}) d_{i} - M_{T}\left(1 - \sum_{j \in F \cup 0, j \neq i} \sum_{o = 1} x_{ijv}^{o}\right) \qquad \forall i \in F, \forall v \in V \tag{A.16}$$

$$q_{iv}^{t} \geq b d_{i} - M_{T}\left(1 - \sum_{j \in F \cup 0, j \neq i} \sum_{o = 2} x_{ijv}^{o}\right) \qquad \forall i \in F, \forall v \in V \tag{A.17}$$

$$x_{ijv}^{o} \in \{0, 1\} \qquad \forall i, j \in F \cup 0, i \neq j, \forall v \in V, \forall o \in O \tag{A.18}$$

$$a_{iv}^{t}, m_{iv}^{t}, n_{iv}^{t}, q_{iv}^{t} \geq 0 \qquad \forall i \in F \cup 0, \forall v \in V \tag{A.19}$$

$$a_{0v}^{t} \leq t_{0}^{l}, l_{0v}^{t} \geq t_{0}^{e} \qquad \forall v \in V \tag{A.20}$$

**Table A1**
Notations of symbols used in model formulation.

| Sets: | |
|---|---|
| $F$ | Set of all orders |
| $V$ | Set of all vehicles |
| $O$ | Set of service types, $O = \{1, 2\}$, where1 "1" represents mobile precooling and "2" denotes centralized precooling |
| **Parameters:** | |
| $\alpha$ | Product decay rate |
| $T(t)$ | Temperature function with time |
| $\alpha(T(t))$ | Decay rate function with temperature |
| $p_i$ | Picking period of order $i$, $i \in F$ |
| $Q(t)$ | Quality decay function with time |
| $Q_{\min}$ | The minimum quality level for products at $t_i^{p}$ promised by PSPs |
| $T_i^{\text{latest}}$ | The latest time for order $i$ to receive precooling services, $i \in F$ |
| $d_{ij}$ | Distance between node $i$ and node $j$, $i,j \in F \cup 0$, where1 "0" represents the central precooling station |
| $t_{ij}$ | Travel time between node $i$ and node $j$, $i,j \in F \cup 0$ |
| $d_i$ | Precooling volume of order $i$, $i \in F$ |
| $[t_i^{e}, t_i^{l}]$ | Time window of order $i$, $i \in F$ |
| $[t_0^{e}, t_0^{l}]$ | Time window of the precooling station |
| $\varphi_1$, $\varphi_2$ | Penalty cost for vehicle waiting or delay for per unit of time |
| $r_{p}$ | Precooling rate of precooling vehicles |
| $b$ | Loading and unloading speed |
| $C_{k}$ | Trucks' maximum load capacity |
| $C_{s}$ | Precooling station's maximum service capacity |
| $T_{\max}$ | Precooling vehicles' maximum working hours |
| $h_{k}$, $h_{r}$, $h_{p}$ | Fixed costs of collecting trucks, refrigerated trucks, and precooling vehicles |
| $f_{k}$, $f_{r}$, $f_{p}$ | Cost per unit distance traveled by collecting trucks, refrigerated trucks, and precooling vehicles |
| $u_{s}$, $u_{p}$ | Cooling cost for handling per unit demand by centralized precooling and mobile precooling |
| **Decision variables:** | |
| $x_{ijv}^{o}$ | If vehicle $v$ belonging to service type $o$ visits from node $i$ to node $j$, $x_{ijv}^{o} = 1$; otherwise$x_{ijv}^{o} = 0$. $i,j \in F \cup 0$, $v \in V$ |
| $a_{iv}^{t}$ | Vehicle $v$'s arrival time to node $i$, $i \in F \cup 0$, $v \in V$ |
| $l_{0v}^{t}$ | Departure time of vehicle v from the precooling station, $v \in V$ |
| $q_{iv}^{t}$ | Vehicle $v$'s service time at order $i$, $i \in F$, $v \in V$ |
| $m_{iv}^{t}$,$n_{iv}^{t}$ | Vehicle $v$'s waiting and delay time at order $i$, $i \in F$, $v \in V$ |
| $t_i^{p}$ | Time when order $i$ receives precooling service, $i \in F$ |
| $q_i^{\text{start\_p}}$ | Quality of order $i$'s products at $t_i^{p}$, $i \in F$ |

## Appendix B

### *B.1. The discretization of the quality decay function*

It has been shown in our preliminary tests that calculating the product quality based on the proposed integral formulations is time-consuming. We therefore develop discretized formulations to approximate the integral formulations while guaranteeing the precision of the results. The main idea is to divide a period into a set of small segments and assume that the temperature in one segment is fixed. Thus, the continuous decay rates in a period under fluctuating temperatures can be represented by a series of discretized decay rates under fixed temperatures. In this study, one hour is divided into 100 segments. Using this kind of approximation, the calculation speed is increased by at least 100 times, while the error is less than 0.05%. Detailed formulations are as follows.

Let $w$ be the number of segments $\Delta t'$ in a period $\Delta t$, and $\Delta t' = \left[t_1^{'j}, t_2^{'j}\right]$ be the $j$th segment. The quality of the product $\Delta t$ after harvest can therefore be represented by $e^{-\Delta t' \sum_{j=1}^{w} \alpha\left(T\left(t_1^{'j}\right)\right)}$.

Furthermore, we define a batch of products as the products picked within a time segment $\Delta t'$ and assume that product quality is consistent in one batch. A discrete way to calculate the product quality $Q_i(t)$ of farmer $i$ at the time $t$ is as follows:

$$Q_i(t) = \frac{1}{N_i^b}\left(1 + \sum_{j=1}^{N_i^b-1} e^{-\Delta t' \sum_{u=j}^{N_i^b-1} \alpha\left(T\left(t_i^e - p_i + \Delta t' u\right)\right)}\right) e^{-\Delta t' \sum_{v=1}^{N_i^c} \alpha\left(T\left(t_i^e + \Delta t'(v-1)\right)\right)} \tag{B.1}$$

where $N_i^b = p_i/\Delta t'$ denotes the number of product batches at farmer $i$, and $N_i^c$ equals $\left(t - t_i^e\right)/\Delta t'$.

### B.2. Pre-processing a quality matrix

This section aims to improve the solution efficiency by calculating the product quality of individual farmers at any possible time in advance. As shown in Eq. (B.1), three inputs are needed to obtain the results, including the picking period and the earliest service time of a request, and any possible start times of precooling to serve the request. Assume that farmers' picking periods are divided into 1, 2, 3, 4, and 5 hours. The earliest service times of orders range from 6:30 am to 11:00 am, which consists of 10 scenarios with an interval of half an hour. The possible start time $t$ of precooling at node $i$ ranges form $t_i^e$ to $T_L$, where $T_L$ denotes the possible latest start time of precooling. We set $T_L$ as two hours after the latest service time $t_0^l$ of the precooling station. For instance, if $t_i^e$ equals 6:30 and $t_0^l$ equals 12:00, there are total 751 possible start times of precooling, because one hour is divided into 100 segments. We therefore obtain a three-dimensional matrix with 26300 ($5 \times (751 + 701 + 651 + 601 + 551 + 501 + 451 + 401 + 351 + 301)$) possible results of the product quality.

It is verified that using the quality matrix can significantly reduce solution times. For 100-customer instances, only 0.4 seconds is required in an iteration, which increases to nearly 40 seconds if the quality matrix is not used. The total time to calculate the quality matrix is no more than 5 minutes.

## Appendix C

This part aims to reveal the impacts of quality decay functions on the mathematical model of the investigated problem. Two distinct quality decay functions are examined, with Method 1 presenting a proposed quality decay function that accounts for varying temperatures and different picking batches (i.e., $Q(t) = \frac{1}{p_i}\int_{t_i^e-p_i}^{t_i^e}\left(e^{-\int_{t'}^{t}\alpha(T(t''))\mathrm{d}t''}\right)\mathrm{d}t'$). Method 2 introduces a simplified quality decay function with fewer inputs, wherein products degradation commences at the midpoint of the picking period, and the temperature remains constant throughout the scheduling period, equal to the average temperature $T_{\text{ave}}$ (i.e., $Q(t) = e^{-\alpha(T_{\text{ave}})\Delta t}$).

Here, mobile precooling is taken as an example. Vehicles are required to arrive at order $i$ before its latest service time $t_i^l$ and ensure that the quality of order $i$'s products at the time ($t_i^p$) of receiving precooling services exceeds the minimum quality level $Q_{\min}$, i.e., $Q\left(t_i^p\right) \geq Q_{\min}$. Based on this formulation, the latest time $T_i^{\text{latest}}$ for order $i$ to receive precooling services can be determined. As a result, the time window constraints at node $i$ are illustrated in Fig. C1.

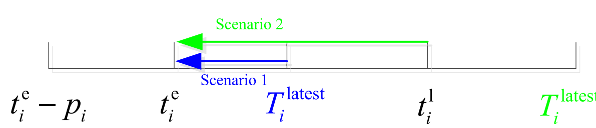


**Fig. C1.** Time window constraints at node $i$ serviced by mobile precooling.

As depicted in Fig. C1, under scenario 1, $T_i^{\text{latest}}$ is earlier than $t_i^l$, indicating that the arrival time $a_{iv}^t$ of vehicle $v$ at node $i$ should satisfy the constraint $t_i^e \leq a_{iv}^t \leq T_i^{\text{latest}}$. Conversely, in scenario 2 where $T_i^{\text{latest}}$ is later than $t_i^l$, $a_{iv}^t$ should satisfy the constraint $t_i^e \leq a_{iv}^t \leq t_i^l$ while $T_i^{\text{latest}}$ does not impose any restrictions on vehicle's arrival time.

Based on the above analysis, a comparison of the two quality decay functions can be conducted under scenario 1. Let $T_i^{\text{latest1}}$ and $T_i^{\text{latest2}}$ represent the latest time for order $i$ to receive precooling services calculated using method 1 and method 2, respectively. When employing method 2, there is a possibility of overestimating or underestimating product quality, consequently resulting in either later or earlier $T_i^{\text{latest}}$ and further relax or tighten time window constraints, as shown in Fig. C2. If $T_i^{\text{latest2}} \geq T_i^{\text{latest1}}$, constraints are relaxed; otherwise, constraints are tightened.

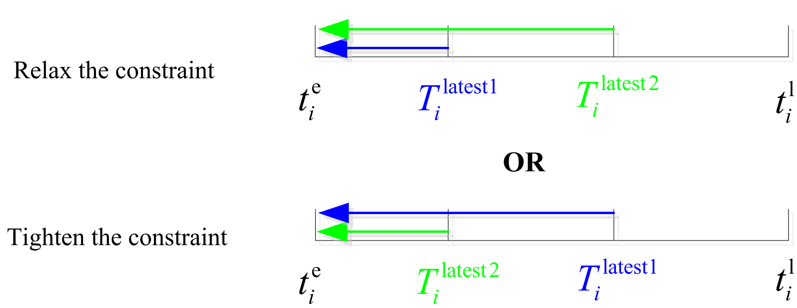


**Fig. C2.** Comparison of the two quality decay functions in relation to time window constraints.

In conclusion, the quality decay function has the potential to alter time window constraints and potentially impact the final scheduling outcomes in scenarios with $T_i^{\text{latest}}$ earlier than $t_i^{\text{l}}$. Six factors that may contribute to $T_i^{\text{latest}} < t_i^{\text{l}}$ are identified based on the quality decay functions, including longer picking period $p_i$, later earliest service time $t_i^{\text{e}}$, higher temperatures $T$ during the scheduling period, higher decay rate $\alpha$, higher minimum quality level $Q_{\min}$, and wider interval between $t_i^{\text{e}}$ and $t_i^{\text{l}}$.

For instance, Table C1 presents the outcomes of $T_i^{\text{latest}}$ computed using two types of quality decay functions across various parameter settings for a single order, with each hour represented by 100. The earliest service time $t_i^{\text{e}}$ for order $i$ is 9:00. The temperature function is based on Eq. (12), encompassing temperatures ranging from 25°C to 37°C. In method 2, the average temperature $T_{\text{ave}}$ corresponds to either the weighted mean temperature (28°C) or the mean temperature (31°C). The decay rate function is $\alpha(T) = 0.0048e^{0.1036T}$, where $\alpha$ takes values of 0.0873 and 0.1191 when the temperature equals 28°C and 31°C, respectively. As indicated in Table C1, in most scenarios, utilizing the quality decay function with fewer inputs results in relaxed or tightened time window constraints.

**Table C1**
Results of $T_i^{\text{latest}}$ calculated using two kinds of quality decay functions.

| $p_i$ | $[t_i^{\text{e}}, t_i^{\text{l}}]$ | $Q_{\min}$ | Method 1 (Using time-varying temperatures) | Method 2 (Using average temperatures) | | Method 2's impacts on time window constraints | |
|---|---|---|---|---|---|---|---|
| | | | $T_i^{\text{latest1}}$ | $T_i^{\text{latest2}}$ ($T_{\text{ave}} = 28^\circ$) | $T_i^{\text{latest2}}$ ($T_{\text{ave}} = 31^\circ$) | $T_{\text{ave}} = 28^\circ$ | $T_{\text{ave}} = 31^\circ$ |
| 1h | [9:00, 10:00] | 85% | 983 | 1036 | 986 | relax | relax |
| | | 80% | 1021 | 1106 | 1037 | —— | —— |
| | [9:00, 11:00] | 85% | 983 | 1036 | 986 | relax | relax |
| | | 80% | 1021 | 1106 | 1037 | relax | relax |
| 2h | [9:00, 10:00] | 85% | 949 | 986 | 936 | relax | tighten |
| | | 80% | 993 | 1056 | 987 | relax | tighten |
| | [9:00, 11:00] | 85% | 949 | 986 | 936 | relax | tighten |
| | | 80% | 993 | 1056 | 987 | relax | tighten |

## Appendix D

**Table D1**
Best results calculated with three state-of-the-art algorithms and the QTDD-based ALNS algorithm on solving large-scale HFVRPTW instances (the number of nodes is 100).

| Instances | Fleet size | Hybrid evolutionary algorithm (Koc et al., 2015) | | Branch-and-check (Fachini & Armentano, 2020) | | Classic ALNS (Lin et al., 2023) | | QTDD-based ALNS | | | Deviations from existing methods | | |
|---|---|---|---|---|---|---|---|---|---|---|---|---|---|
| | | Cost | Vehicle | Cost | Vehicle | Cost | Vehicle | Cost | Vehicle | Average costs | Dev1 | Dev2 | Dev3 |
| R101A | $A^1B^{11}C^{11}D^1$ | 4355.41 | $B^{10}C^{11}D^1$ | 4417.59 | $A^1B^{10}C^{11}D^1$ | 4455.40 | $A^1B^{10}C^{11}D^1$ | 4429.18 | $A^1B^{10}C^{11}D^1$ | 4473.10 | 1.69% | 0.26% | -0.59% |
| R102A | $A^1B^4C^{14}D^2$ | 4356.44 | $B^4C^{13}D^2$ | 4262.97 | $A^1B^2C1^4D^2$ | 4359.69 | $B^3C^{14}D^2$ | 4329.48 | $B^3C^{14}D^2$ | 4354.78 | -0.62% | 1.56% | -0.69% |
| R103A | $B^7C^{15}$ | 4080.16 | $B^6C^{15}$ | 4092.43 | $B^6C^{15}$ | 4187.53 | $B^6C^{15}$ | 4139.48 | $B^6C^{15}$ | 4161.88 | 1.45% | 1.15% | -1.15% |
| R104A | $B^9C^{14}$ | 3954.72 | $B^7C^{14}$ | 4024.82 | $B^9C^{13}$ | 4081.94 | $B^7C^{14}$ | 4036.68 | $B^7C^{14}$ | 4082.00 | 2.07% | 0.29% | -1.11% |
| R201A | $A^5$ | 3448.76 | $A^5$ | 3539.83 | $A^5$ | 3514.88 | $A^5$ | 3489.23 | $A^5$ | 3526.54 | 1.17% | -1.43% | -0.73% |
| R202A | $A^5$ | 3308.16 | $A^5$ | 3441.36 | $A^5$ | 3385.92 | $A^5$ | 3323.46 | $A^5$ | 3357.81 | 0.46% | -3.43% | -1.84% |
| R203A | $A^4B^1$ | 3382.39 | $A^4B^1$ | 3586.58 | $A^4B^1$ | 3438.84 | $A^4B^1$ | 3407.46 | $A^4B^1$ | 3438.79 | 0.74% | -4.99% | -0.91% |
| R204A | $A^5$ | 3018.14 | $A^5$ | 3145.57 | $A^5$ | 3068.83 | $A^5$ | 3054.12 | $A^5$ | 3072.05 | 1.19% | -2.91% | -0.48% |
| C101A | $A^1B^{10}$ | 8828.94 | $B^{10}$ | 8828.94 | $B^{10}$ | 8828.94 | $B^{10}$ | 8828.94 | $B^{10}$ | 8828.94 | 0.00% | 0.00% | 0.00% |
| C102A | $A^{19}$ | 7080.17 | $A^{19}$ | 7106.53 | $A^{19}$ | 7113.40 | $A^{19}$ | 7084.88 | $A^{19}$ | 7128.24 | 0.07% | -0.30% | -0.40% |
| C103A | $A^{19}$ | 7079.21 | $A^{19}$ | 7079.22 | $A^{19}$ | 7176.07 | $A^{19}$ | 7082.65 | $A^{19}$ | 7099.40 | 0.05% | 0.05% | -1.30% |
| C104A | $A^{19}$ | 7075.06 | $A^{19}$ | 7097.86 | $A^{19}$ | 7199.45 | $A^{19}$ | 7077.44 | $A^{19}$ | 7113.46 | 0.03% | -0.29% | -1.69% |
| C201A | $A^4B^1$ | 6082.38 | $A^4B^1$ | 6082.38 | $A^4B^1$ | 6102.26 | $A^4B^1$ | 6085.42 | $A^4B^1$ | 6107.10 | 0.05% | 0.05% | -0.28% |
| C202A | $A^1C^3$ | 7618.62 | $A^1C^3$ | 7639.79 | $A^1C^3$ | 7636.74 | $A^1C^3$ | 7618.62 | $A^1C^3$ | 7621.11 | 0.00% | -0.28% | -0.24% |
| C203A | $C^2D^1$ | 7303.37 | $C^2D^1$ | 7401.30 | $C^2D^1$ | 7385.28 | $C^2D^1$ | 7320.20 | $C^2D^1$ | 7345.13 | 0.23% | -1.10% | -0.88% |
| C204A | $A^5$ | 5677.66 | $A^5$ | 5935.47 | $A^5$ | 5693.28 | $A^5$ | 5682.88 | $A^5$ | 5721.67 | 0.09% | -4.26% | -0.18% |
| RC101A | $A^7B^7C^7$ | 5162.28 | $A^4B^7C^7$ | 5298.36 | $A^5B^7C^7$ | 5305.29 | $A^5B^7C^7$ | 5298.62 | $A^5B^7C^7$ | 5312.48 | 2.64% | 0.00% | -0.13% |
| RC102A | $A^5B^6C^8$ | 5018.05 | $A^2B^6C^8$ | 5148.72 | $A^3B^6C^8$ | 5158.97 | $A^4B^5C^8$ | 5121.41 | $A^4B^5C^8$ | 5196.22 | 2.06% | -0.53% | -0.73% |
| RC103A | $A^{11}B^2C^8$ | 4926.55 | $A^{10}B^2C^8$ | 4998.63 | $A^{10}B^2C^8$ | 5144.77 | $A^{10}B^2C^8$ | 5074.25 | $A^{10}B^2C^8$ | 5187.48 | 3.00% | 1.51% | -1.37% |
| RC104A | $A^2B^{13}C^3D^1$ | 4995.91 | $A^2B^{13}C^3D^1$ | 5050.02 | $A^2B^{13}C^3D^1$ | 5168.46 | $A^2B^{13}C^3D^1$ | 5129.32 | $A^2B^{13}C^3D^1$ | 5199.76 | 2.67% | 1.57% | -0.76% |
| RC201A | $C^1E^3$ | 5344.47 | $C^1E^3$ | 5395.99 | $C^1E^3$ | 5313.25 | $C^1E^3$ | 5313.25 | $C^1E^3$ | 5389.71 | -0.58% | -1.53% | 0.00% |
| RC202A | $A^1C^1D^1E^2$ | 4856.02 | $A^1C^1D^1E^2$ | 5166.76 | $A^1C^1D^1E^2$ | 5156.71 | $A^1C^1D^1E^2$ | 4920.09 | $A^1C^1D^1E^2$ | 4963.52 | 1.32% | -4.77% | -4.59% |
| RC203A | $A^1B^1C^5$ | 4246.25 | $A^1B^1C^5$ | 4424.82 | $A^1B^1C^5$ | 4361.26 | $A^1B^1C^5$ | 4277.18 | $A^1B^1C^5$ | 4364.54 | 0.73% | -3.34% | -1.93% |
| RC204A | $A^{14}B^2$ | 4195.32 | $A^{14}B^2$ | 4410.37 | $A^{14}B^2$ | 4379.14 | $A^{14}B^2$ | 4225.24 | $A^{14}B^2$ | 4301.80 | 0.71% | -4.20% | -3.51% |
| Ave | | **5.45** | | **179.68** | | **6.97** | | **5.24** | | | **0.88%** | **-1.12%** | **-1.06%** |
| Runs | | 10 | | 1 | | 20 | | 10 | | | | | |
| Processor | | Intel Xeon 2.6GHz | | Intel Core i7 2.5GHz | | Intel Core i5 1.60GHz | | Intel Core i5 1.60GHz | | | | | |

## References


Akkerman, R., Farahani, P., & Grunow, M. (2010). Quality, safety and sustainability in food distribution: a review of quantitative operations management approaches and challenges. *OR Spectrum, 32*(4), 863–904. https://doi.org/10.1007/s00291-010-0223-2

Albrecht, W., & Steinrucke, M. (2018). Coordinating continuous-time distribution and sales planning of perishable goods with quality grades. *International Journal of Production Research, 56*(7), 2646–2665. https://doi.org/10.1080/00207543.2017.1384584

Alvarez, A., Cordeau, J. F., Jans, R., Munari, P., & Morabito, R. (2020). Formulations, branch-and-cut and a hybrid heuristic algorithm for an inventory routing problem with perishable products. *European Journal of Operational Research, 283*(2), 511–529. https://doi.org/10.1016/j.ejor.2019.11.015

Alvarez, A., Miranda, P., & Rohmer, S. U. K. (2022). Production routing for perishable products. *Omega-International Journal of Management Science, 111*, Article 102667. https://doi.org/10.1016/j.omega.2022.102667

Amorim, P., & Almada-Lobo, B. (2014). The impact of food perishability issues in the vehicle routing problem. *Computers & Industrial Engineering, 67*, 223–233. https://doi.org/10.1016/j.cie.2013.11.006

Baranyai, L., Lien Le Phuong, N., Dam, M. S., Zsom, T., & Hitka, G. (2020). Evaluation of precooling temperature and 1-MCP treatment on quality of 'Golden Delicious' apple. *Journal of Applied Botany and Food Quality, 93*, 130–135. https://doi.org/10.5073/JABFQ.2020.093.017

Blackburn, J., & Scudder, G. (2009). Supply chain strategies for perishable products: The case of fresh produce. *Production and Operations Management, 18*(2), 129–137. https://doi.org/10.1111/j.1937-5956.2009.01016.x

Bogataj, D., Bogataj, M., & Hudoklin, D. (2017). Mitigating risks of perishable products in the cyber-physical systems based on the extended MRP model. *International Journal of Production Economics, 193*, 51–62. https://doi.org/10.1016/j.ijpe.2017.06.028

Chen, H. K., Hsueh, C. F., & Chang, M. S. (2009). Production scheduling and vehicle routing with time windows for perishable food products. *Computers & Operations Research, 36*(7), 2311–2319. https://doi.org/10.1016/j.cor.2008.09.010

Chen, J. Y., Fan, T. J., & Pan, F. (2021). Urban delivery of fresh products with total deterioration value. *International Journal of Production Research, 59*(7), 2218–2228. https://doi.org/10.1080/00207543.2020.1828638

de Keizer, M., Akkerman, R., Grunow, M., Bloemhof, J. M., Haijema, R., & van der Vorst, J (2017). Logistics network design for perishable products with heterogeneous quality decay. *European Journal of Operational Research, 262*(2), 535–549. https://doi.org/10.1016/j.ejor.2017.03.049

de Keizer, M., Haijema, R., Bloemhof, J. M., & van der Vorst, J (2015). Hybrid optimization and simulation to design a logistics network for distributing perishable products. *Computers & Industrial Engineering, 88*, 26–38. https://doi.org/10.1016/j.cie.2015.06.017

Duan, Y., Wang, G. B., Fawole, O. A., Verboven, P., Zhang, X. R., Wu, D., . . . Chen, K. S. (2020). Postharvest precooling of fruit and vegetables: A review. *Trends in Food Science & Technology*, 100, 278-291. https://doi.org/10.1016/j.tifs.2020.04.027.

Fachini, R. F., & Armentano, V. A. (2020). Logic-based Benders decomposition for the heterogeneous fixed fleet vehicle routing problem with time windows. *Computers & Industrial Engineering, 148*, Article 106641. https://doi.org/10.1016/j.cie.2020.106641

Fikar, C. (2018). A decision support system to investigate food losses in e-grocery deliveries. *Computers & Industrial Engineering, 117*, 282–290. https://doi.org/10.1016/j.cie.2018.02.014

Gaukler, G. M., Zuidwijk, R. A., & Ketzenberg, M. E. (2023). The value of time and temperature history information for the distribution of perishables. *European Journal of Operational Research, 310*(2), 627–639. https://doi.org/10.1016/j.ejor.2023.03.006

Gomez-Lagos, J. E., Gonzalez-Araya, M. C., Soto-Silva, W. E., & Rivera-Moraga, M. M. (2021). Optimizing tactical harvest planning for multiple fruit orchards using a metaheuristic modeling approach. *European Journal of Operational Research, 290*(1), 297–312. https://doi.org/10.1016/j.ejor.2020.08.015

Gustavsson, J., Cederberg, C., Sonesson, U., Van Otterdijk, R., & Meybeck, A. (2011). *Global food losses and food waste*, 2023. http://www.fao.org/docrep/014/mb060e/mb060e.pdf Accessed April 21.

Han, J. L., Lin, N., Ruan, J. H., Wang, X. P., Wei, W., & Lu, H. M. (2021). A model for joint planning of production and distribution of fresh produce in agricultural Internet of Things. *IEEE Internet of Things Journal, 8*(12), 9683–9696. https://doi.org/10.1109/JIOT.2020.3037729

Koc, C., Bektas, T., Jabali, O., & Laporte, G. (2015). A hybrid evolutionary algorithm for heterogeneous fleet vehicle routing problems with time windows. *Computers & Operations Research, 64*, 11–27. https://doi.org/10.1016/j.cor.2015.05.004

Lawrence, B., & Melgar, J. C. (2018). Harvest, handling, and storage recommendations for improving postharvest quality of blackberry cultivars. *Horttechnology, 28*(5), 578–583. https://doi.org/10.21273/HORTTECH04062-18

Lejarza, F., & Baldea, M. (2022). An efficient optimization framework for tracking multiple quality attributes in supply chains of perishable products. *European Journal of Operational Research, 297*(3), 890–903. https://doi.org/10.1016/j.ejor.2021.04.057

Lejarza, F., & Baldea, M. (2020). Closed-loop optimal operational planning of supply chains with fast product quality dynamics. *Computers & Chemical Engineering, 132*, Article 106594. https://doi.org/10.1016/j.compchemeng.2019.106594

Lejarza, F., Pistikopoulos, I., & Baldea, M. (2021). A scalable real-time solution strategy for supply chain management of fresh produce: A Mexico-to-United States cross border study. *International Journal of Production Economics, 240*, Article 108212. https://doi.org/10.1016/j.ijpe.2021.108212

Lin, N., Akkerman, R., Kanellopoulos, A., Hu, X., Wang, X., & Ruan, J. (2023). Vehicle routing with heterogeneous service types: Optimizing post-harvest preprocessing operations for fruits and vegetables in short food supply chains. *Transportation Research Part E: Logistics and Transportation Review, 172*, Article 103084. https://doi.org/10.1016/j.tre.2023.103084

Liu, F. H., & Shen, S. Y. (1999). The fleet size and mix vehicle routing problem with time windows. *Journal of the Operational Research Society, 50*(7), 721–732. https://doi.org/10.1057/palgrave.jors.2600763

Kitinoja, L., & Thompson, J. F. (2010). Pre-cooling systems for small-scale producers. *Stewart Postharvest Review, 6*(2), 1–14.

Li, Y., Wang, X., Lin, N., Feng, X., Ruan, J., & Hu, X. (2022). The location-routing optimization model and algorithm of multi-type precooling facilities for agricultural products. *Systems Engineering-Theory & Practice, 42*(11), 3016–3029.

Mercier, S., Villeneuve, S., Mondor, M., & Uysal, I. (2017). Time-temperature management along the food cold chain: A review of recent developments. *Comprehensive Reviews in Food Science and Food Safety, 16*(4), 647–667. https://doi.org/10.1111/1541-4337.12269

Han, J. W., Zuo, M., Zhu, W. Y., Zuo, J. H., Lu, E. L., & Yang, X. T. (2021). A comprehensive review of cold chain logistics for fresh agricultural products: Current status, challenges, and future trends. *Trends in Food Science & Technology*, 109, 536-551. https://doi.org/10.1016/j.tifs.2021.01.066.

MOA. (2023). Field research: Post-harvest precooling techniques for preserving the quality of asparagus. Ministry of Agriculture and Rural Affairs of the People's Republic of China. http://www.scs.moa.gov.cn/ccll/tpxw/202302/t20230206_6419936.htm. Accessed May 15, 2024.

Pasandideh, S. H. R., Rahbari, M., & Sadati-Keneti, Y. (2023). A Lagrangian relaxation algorithm and hybrid genetic algorithm-black widow optimization for perishable products supply chain with sustainable development goals consideration. *Annals of Operations Research.* https://doi.org/10.1007/s10479-023-05532-x Accessed September 01, 2024.

Pelletier, W., Brecht, J. K., Nunes, M. C. D., & Émond, J. P. (2011). Quality of strawberries shipped by truck from California to Florida as influenced by postharvest temperature management practices. *Horttechnology, 21*(4), 482–493. https://doi.org/10.21273/horttech.21.4.482

Rodriguez, P. (2021). Mobile pre-cooling on-the-go. https://www.inspirafarms.com/mobile-precooling-on-the-go/. Accessed May 15, 2024.

Rong, A. Y., Akkerman, R., & Grunow, M. (2011). An optimization approach for managing fresh food quality throughout the supply chain. *International Journal of Production Economics, 131*(1), 421–429. https://doi.org/10.1016/j.ijpe.2009.11.026

Ruan, J. H., Hu, X. P., Huo, X. X., Shi, Y., Chan, F. T. S., Wang, X. P., … Zhao, X. F (2020). An IoT-based E-business model of intelligent vegetable greenhouses and its key operations management issues. *Neural Computing & Applications, 32*(19), 15341–15356. https://doi.org/10.1007/s00521-019-04123-x

Shaw, P. (1997). *A new local search algorithm providing high quality solutions to vehicle routing problems. Technical report.* Scotland: Department of Computer Science, University of Strathclyde.

Stellingwerf, H. M., Groeneveld, L. H. C., Laporte, G., Kanellopoulos, A., Bloemhof, J. M., & Behdani, B. (2021). The quality-driven vehicle routing problem: Model and application to a case of cooperative logistics. *International Journal of Production Research, 231*, Article 107849. https://doi.org/10.1016/j.ijpe.2020.107849

Tsang, Y. P., Wu, C. H., Lam, H. Y., Choy, K. L., & Ho, G. T. S. (2021). Integrating Internet of Things and multi-temperature delivery planning for perishable food E-commerce logistics: a model and application. *International Journal of Production Research, 59*(5), 1534–1556.

Vigneault, C., Gariepy, Y., Roussel, D., & Goyette, B. (2004). The effect of precooling delay on the quality of stored sweet corn. *Journal of Food Agriculture & Environment, 2*(2), 71–73. https://doi.org/10.1016/S1389-1723(04)70206-6

Wang, X., Wang, Y., Li, Y., & Lin, N. (2024). Collaborative scheduling of grading and pre-cooling vehicles for post-harvest fruits and vegetables: Model formulations and solution algorithms. *Journal of Systems & Management, 33*(1), 76–89.

Yang, C., Lan, S. L., Zhao, Z. H., Zhang, M. D., Wu, W., & Huang, G. Q. (2023). Edge-cloud blockchain and IoE-enabled quality management platform for perishable supply chain logistics. *IEEE Internet of Things Journal, 10*(4), 3264–3275. https://doi.org/10.1109/JIOT.2022.3142095

Yang, C. Y., Feng, Y. H., & Whinston, A. (2022). Dynamic pricing and information disclosure for fresh produce: An artificial intelligence approach. *Production and Operations Management, 31*(1), 155–171. https://doi.org/10.1111/poms.13525

Zhu, H. L., Liu, C. C., Wu, G. H., & Gao, Y. J. (2023). Cold chain logistics network design for fresh agricultural products with government subsidy. *Sustainability, 15*(13), 10021. https://doi.org/10.3390/su151310021

Zhao, H. X., Liu, S., Tian, C. Q., Yan, G., & Wang, D. (2018). An overview of current status of cold chain in China. *International Journal of Refrigeration, 88*, 483–495. https://doi.org/10.1016/j.ijrefrig.2018.02.024